Fabrication and Characterization of Blends of P(VDF-CTFE) 91/9 and PMMA

by

Jialiang Shen

A thesis submitted to the Graduate Faculty of
Auburn University
in partial fulfillment of the
requirements for the Degree of
Master of Science

Auburn, Alabama
May 4, 2019

Keywords: Dielectric materials, blends, dielectric constant, dielectric loss, energy-storage density, DSC

Approved by

Zhongyang Cheng, Chair, Professor of Materials Engineering
Pengyu Chen, Assistant Professor of Materials Engineering
Edward Davis, Assistant Professor of Materials Engineering

ABSTRACT

Transparent and flexible polymer blends with a uniform thickness of films about 8 microns were successfully and simply fabricated by a spin-coating method. PMMA polymer and P(VDF-CTFE) 91/9 mol. % (VC91) copolymer were mixed and dissolved in DMF solvent, with different volume fraction of PMMA from 0 vol. % to 100 vol. %. Dielectric properties, polarization-electric field (P-E) hysteresis loops and differential scanning calorimetry (DSC) were measured in this study. At room temperature, dielectric constant decreased, while dielectric loss decreased at low frequency and increased at high frequency, with increasing volume fraction of PMMA. Temperature dependence of dielectric properties were investigated and explained by several relaxation processes. With increasing PMMA content, breakdown fields increased, and maximal polarization and remnant polarization decreased. Energy-storage performances were calculated from P-E loops. Maximum charged and discharged energy density were about 26.4 J/cm^3 and 10.4 J/cm^3, obtaining in PMMA-VC91 blends with 10 vol. % and 30 vol. % of PMMA, respectively. Also, efficiency increased as the addition of PMMA. The phase transitions, such as glass transition, fusion, crystallization, were investigated by DSC, assisting to understand the dielectric behaviors of PMMA-VC91 blends.

ACKNOWLEDGMENTS

I would like to deeply appreciate my advisor Dr. Zhongyang Cheng, who helped and guided me for my graduate studies in Auburn university. His patient instruction and encouragement were invaluable for me to complete my research study and to pursue my future career.

I want to give my gratitude to my committee members, Dr. Pengyu Chen and Dr. Edward Davis, for their kind suggestions and helps in my graduation thesis and oral defense.

I also express my appreciation to my group members, Dr. Xu Lu, Dr. Zhuo Wang, Jindong Wei, Jiachen Liu, Liangxi Li, Yang Tong, Wei Yi, Weiye Wang, Yancen Cai, Hossein Talebinezhad, Farrukh Najmi. Their helps and suggestions played a significant role in my achievement of research. Special thanks to Dr. Xu Lu, he trained me in fabrication and measurement of dielectric materials, and we had a happy cooperation.

Finally, I want to give the sincerest thanks to my parents for their encouragement, support and love during the time that I was pursuing my master's degree.

TABLE OF CONTENTS

LIST OF TABLES

LIST OF FIGURES

CHAPTER 1

INTRODUCTION OF DIELECTRICS

1.1 Dielectric materials

Dielectric materials are usually so-called insulator which has very low electric conductivity, but typically having a high polarization. The term insulator means that it can obstruct direct current to pass through, however the alternating current is allowed flowing through the insulator. That is the reason we name it as dielectric which is widely used in electronic industry to produce electronic and electrical devices such as capacitor [1]. It is one of the most well-known devices which partially consist of dielectric materials, acting as signal filters, charge storages, energy sources and so on.

For different applications, diverse requirements of the performances of dielectric materials are needed. For instance, low dielectric constant materials are preferable to produce integrated circuit and high dielectric constant materials are desirably used in field-effect transistors [2]. Therefore, some basic properties of dielectric materials, such as complex permittivity (ε^*), polarization-electric field (P-E) loop and breakdown field (E_b), need to be tested for characterization in order to find suitable applications of the dielectric materials. Generally, dielectric materials with low loss and high breakdown field can be applied in a high electric field situation and the materials with low dielectric constant can be used in some applications under low electric field. Besides, in some cases, the dielectric

properties with less dependence on temperature influence are required [3]. Therefore, this paper will characterize above properties of materials we developed.

1.2 Theory of dielectrics

1.2.1 Capacitance

If a voltage, V, is applied to two parallel electrodes of a capacitor, there will be some electric charges on the electrodes after cutting off the voltage, as shown in Figure 1.1. In order to characterize the ability of the capacitor to store charges, the capacitance, C, is defined to describe the ability which is the remained charge, q, per unit applied voltage, V, as equation (1.1):

$$C = \frac{q}{V} \tag{1.1}$$

where C has a unit in coulombs per volt or farad.

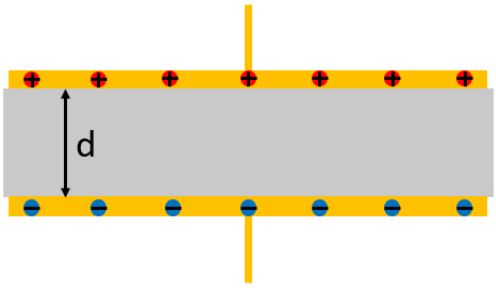

Figure 1. 1 Schematics of a capacitor with a dielectric between two electrodes

The capacitance of a capacitor is also changed by its parameters, such as area of electrodes, A, and the distance between two electrodes, d. It is no doubt that the

dielectric material between two electrodes also significantly affects the capacitance, C, and the relationship is shown as:

$$C = \varepsilon_r \varepsilon_0 \frac{A}{d} \tag{1.2}$$

where ε_r is called dielectric constant or relative permittivity, and it is a unitless value.

Table 1. 1 Dielectric constants under DC voltage at room temperature [4]

Materials	Dielectric constant
Dry air	1.007
Ice	3
Water	81.1
Acetone	20
Marble	8.5
Industrial Alcohol	16-31
PVC	3.5
Silicon	11.8
Alumina	9.3-11.5
Benzene	2.3
$NaKC_4H_4O_6 \cdot 4H_2O$	170
GaAs	10.9
$BaTiO_3$	4000

The ε_0 means the permittivity of vacuum, and usually is a constant which has value of $8.854187817\times10^{-12}$ F/m [4]. There are some values of dielectric constant for some materials shown in Table 1.1 under direct current situation. It is worth mentioning that dielectric constant is dependent on frequency of the applied voltage.

The above information tells us that dielectric materials is very important to the ability of charge or energy storage for a capacitor due to the large difference of their dielectric constant. However, the electric charge will flow away if the dielectric material is penetrated by the voltage, in other word, the applied voltage is higher than the breakdown field. Therefore, the breakdown field of materials is also needed to be considered to build an excellent capacitor with good performance of energy storage.

1.2.2 Dielectrics

This section will introduce some dielectric properties and fundamentals. For better understanding, an electric dipole model, shown as Figure 1.2, needs to be explained first.

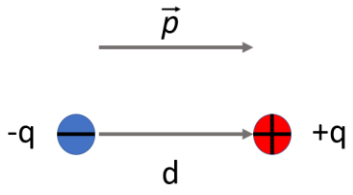

Figure 1. 2 Schematics of an electric dipole

As shown in Figure 1.2, two separated electric charges with same value of charges, q, but opposite sign, have a distance, d, to generate a dipole moment, $\vec{p}$. The electric dipole moment has a magnitude, $p = qd$, with the unit in coulomb·meter (C·m) or debye (D). It is worth mentioning that the direction of a dipole moment is from negative to positive charge.

For an ideal insulator, no current passes through the material under an external direct current electric field, instead of generating a polarization, $\vec{P}$, in the material. Dielectric polarization $\vec{P}$ means electric dipole density per unit volume, as below.

$$\vec{P} = \frac{d\vec{p}}{dV} \tag{1.3}$$

where $d\vec{p}$ is an infinitesimal dipole moment inside of an infinitesimal volume dV. Then, the unit of dielectric polarization $\vec{P}$ is coulomb/m^2 (C/m^2). So, the dielectric polarization also describes polarization charges on the surface of the dielectric materials, shown as figure 1.3.

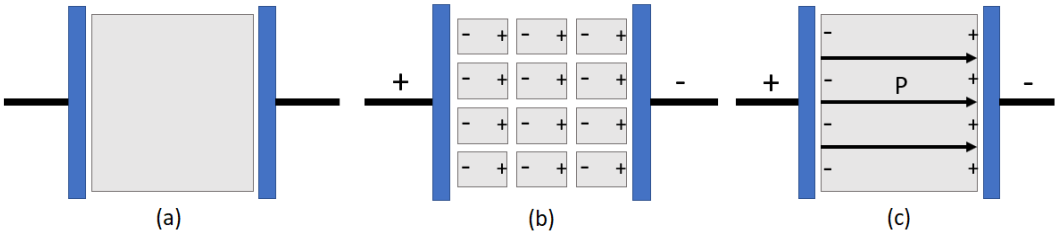

Figure 1. 3 Schematic representation of polarization process of a dielectric material between two electrodes. (a) Dielectric material without an external voltage. (b) The material with induced electric dipoles under an applied voltage. (c) Dielectric polarization and its direction from negative to positive charges.

Figure 1.3 (b) shows infinitesimal dipole moments are induced, and then induced positive and negative charges are neutralized within the dielectric material as Figure 1.3 (c). Therefore, as we discussed previously, dielectric polarization represents the density of induced charges on the surface of the material [4][5].

According to our electromagnetic knowledge, a material exhibits above polarization process under an external electric field $\vec{E}$ defined by an equation as following [4].

$$\vec{D} = \varepsilon_0 \vec{E} + \vec{P} \tag{1.4}$$

where $\vec{D}$ is electric displacement, ε_0 is so-called permittivity in vacuum with the value of $8.854187817\times10^{-12}$ F/m and dielectric polarization $\vec{P}$ was talked previously. The equation (1.4) also can be expressed by

$$\vec{D} = \varepsilon \vec{E} = \varepsilon_r \varepsilon_0 \vec{E} \tag{1.5}$$

where ε_r is mentioned above as dielectric constant and ε is defined as permittivity of this material. Combining equation (1.4) and (1.5), dielectric polarization $\vec{P}$ can be shown as

$$\vec{P} = (\varepsilon_r - 1)\, \varepsilon_0 \vec{E} \tag{1.6}$$

Above discussions and equations are based on DC conditions. In AC conditions, in other words, the dielectric material is applied by a time-varying electric field, these discussions and equations are still consistent and, usually, ε_r and ε are replaced with complex forms into equation (1.5) and (1.6), such as ε_r^* and ε^*, respectively.

As we know, complex parameters can be separated into real part and imaginary part. Therefore, the relative permittivity or dielectric constant with complex form can be expressed as below

$$\varepsilon_r^* = \varepsilon_r' - j\varepsilon_r'' \tag{1.7}$$

where ε_r' is the real part of dielectric constant and ε_r'' is the imaginary part.

So, electric displacement $\vec{D}$ has a different phase with electric field $\vec{E}$ because ε^* is complex under AC condition, which causes the electromagnetic energy dissipation. The dielectric loss can be defined as following relation to describe this energy loss.

$$tan\delta = \frac{\varepsilon_r''}{\varepsilon_r'} \tag{1.8}$$

where $tan\delta$ is called as dielectric loss and δ is the phase angle between the real and imaginary parts of dielectric constant.

1.2.3 Mechanism of polarization

In last section, dipole moment and polarization process were simply discussed. The mechanism of polarization will be deeply introduced as four mechanisms which can explain the polarization response based on the understanding in very small scale of homogeneous materials, such as atoms, molecules or microstructure.

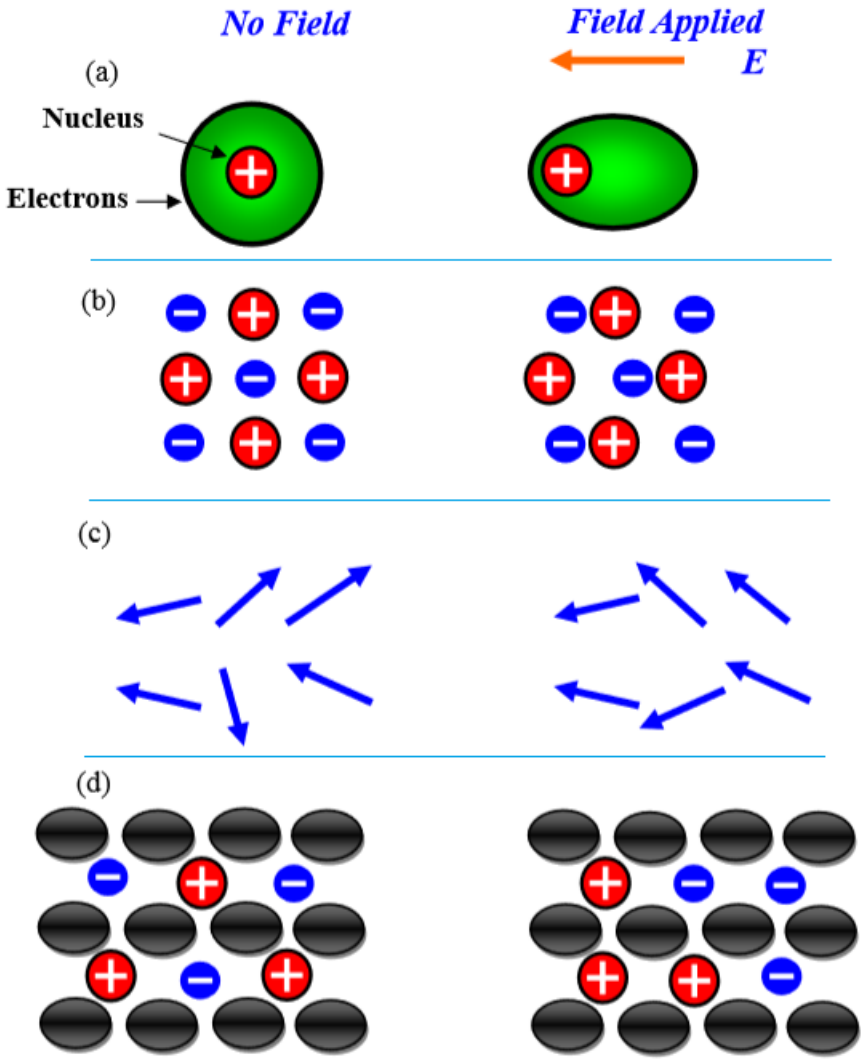

Figure 1. 4 Schematics of four mechanisms in polarization process. (a) eletronic polarization, (b) atomic/ionic polarization, (c) orientational polarization and (d) space charge polarization [8].

Electronic polarization process is shown in Figure 1.4 (a), the green area is the electron cloud which has a displacement from positive nucleus under an external electric field. The response time of the electronic polarization is around 10^{-14} to 10^{-16} s with independence of temperature.

Figure 1.4 (b) shows the atomic/ionic polariztion process under applied voltage. The distance between cation and anion is changed with the electric field. The ionic polarization has a response time of 10^{-12} to 10^{-13} s and the ions response almost has temperature dependence.

The schematic of orientational polarization process is introduced in Figure 1.4 (c). These arrows means dipoles, so that the orientational polarization has to be oberved in materials with dipoles. Under an electric field, a torque is generated and applied on each dipole, which leads dipoles align along the direction of electric field as the right image of Figure 1.4 (c). However, its response time is strongly dependent on temperature and materials with about 10^{0} to 10^{-8} s response.

The last mechanism is called space charge polarization (Figure 1.4 (d)) which appears in a dielectric material with space charges. Applying an electric field, a force is generated on particles to separate positive and negative charges forming some dipole moments in the dielectric material. The response time is greater than 10^{-4} s with a strong temperature dependence.

Figure 1.5 shows the real and imaginary parts of dielectric constant with frequency dependence affected by four polarization responses. Generally speaking, these four polarization mechanisms dominate different frequency ranges. Beside, the electronic and ionic polarization cause a dielectric response, but a relaxation polarization is led by orientational polarization and space charge polarization. By the way, if the frequency is much smaller than 1/t where t is the response time, dielectric constant will become static permitivity with zero imaginary part [8][11].

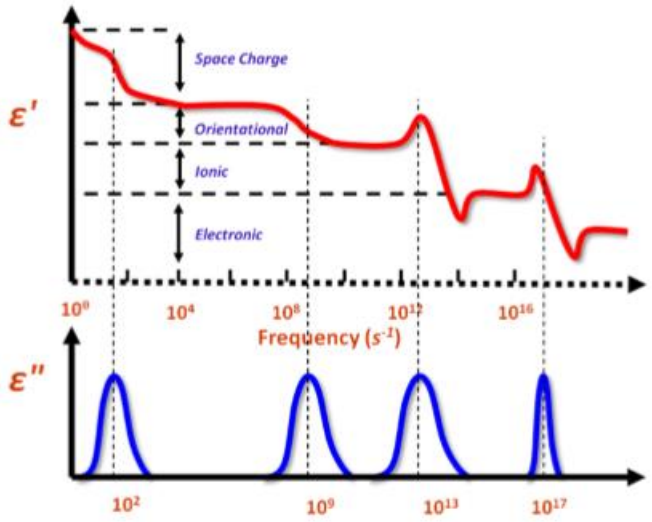

Figure 1. 5 Frequency influence on the real and imaginary part of relative permittivity of a dielectric material based on four different mechanisms [11].

1.3 Classification of dielectric materials

There are many different types of dielectric materials applying in current industry. Due to some applications, gases, liquids and solids are all used as dielectric materials to obtain the specific dielectric properties. So, dielectric materials were classified by different methods in order to apply and understand them better.

The first method is the most basic one to classify dielectric materials into three states: gases, liquids and solids.

Second, Electronic Industries Alliance (EIA) classified dielectric materials into three categories by their dielectric constants. Type I is the dielectric materials with low dielectric constants between 15 – 500, the dielectric loss is not more than 0.003

and their working temperature is in the range of -55 °C and 85 °C. Type II is the dielectric materials have high dielectric constants which are from 500 to 20000. Type III is conductive phase based dielectric materials which possess extremely high capacitance and very low dielectric strength (breakdown field) [7].

Table 1. 2 Common inorganic and organic dielectric materials [7][8][9]

Classification	Names	Dielectric constant	Breakdown field (MV/m)
Inorganic	Air	1.007	3
	Tantalum oxide	11	4
	Fused quartz	3.85	20
	Reconstitute mica	7.8	64
	High-voltage ceramic	500-6000	2
Organic	Epoxy	4	16
	PVDF	11-14	770
	Polyester	2.8-4.5	32
	PSF	3.2	100
	PP	2.3	140
	PI	3.6	339
	PE	2.2-2.4	50

Third, dielectric materials also can be classified by their composition into inorganic and organic dielectric materials. There are some common inorganic and

organic dielectrics with their dielectric constant and breakdown field showing in Table 1.2.

Finally, dielectric materials also can be classified into nonpolar or polar materials [10]. Dielectric materials with no permanent dipole moments are defined as nonpolar materials, which have relatively low relative permittivity comparing with polar materials. Oppositely, materials with a permanent dipole moment are named polar materials. However, some polar materials which have dipoles aligning along a same direction without an external electric field, that causes a spontaneous polarization. These types of materials are called as pyroelectric material. Some of pyroelectric materials, which have the spontaneous polarization that can be switched to the direction along with an external electric field, are named as ferroelectric materials [4].

As we discussed, ferroelectric materials have the spontaneous polarization switched under applied field, so they have very high dielectric constant comparing with other nonpolar or polar materials. Therefore, ferroelectric materials, both inorganic and organic, such as $BaTiO_3$, PVDF and PVDF based copolymers, are focused by many researches to develop dielectric materials with high dielectric constant.

1.4 Energy-storage density

Energy-storage density is a physic characteristic used to describe the ability that a dielectric material can store electric energy under an electric field. It is defined as

$$U = \int_0^D \vec{E} \cdot d\vec{D} \tag{1-9}$$

where U is called energy-storage density which has a unit J/m^3 or J/cm^3, $\vec{E}$ is applied electric field and $\vec{D}$ is electric displacement under applied field $\vec{E}$ [12]. The energy-storage density is expressed in Figure 1.6 with blue areas. Figure 1.6 (a), (b) and (c) exhibit energy-storage density U when electric displacement and field have linear, positive curvature and negative curvature relationship, respectively.

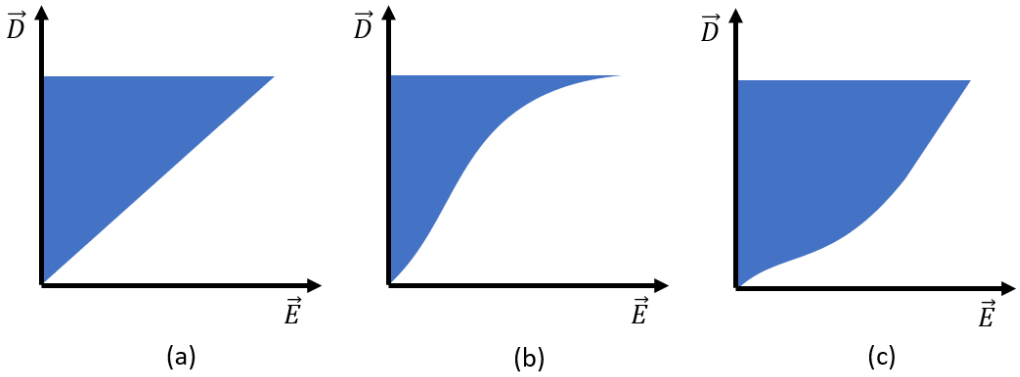

Figure 1. 6 The schematic of energy-storage density in plot of electric displacement vs. electric field.

For easier understanding of the relationship between energy-storage density U and dielectric parameters, such as electric field $\vec{E}$ and dielectric constant ε_r, an equation (1-10) can be simplified based on Figure 1.6 (a) and equation (1-9) in an ideal linear dielectric material [13].

$$U = \frac{1}{2}\varepsilon_r'\varepsilon_0\vec{E}^2 \tag{1-10}$$

Relied on equation (1-10), it is proved that (real part of) dielectric constant and electric field are the most significant factors influencing the energy-storage density

of a dielectric materials. By the way, this equation is simplified model which did not consider the curvature of the relationship between $\vec{D}$ and $\vec{E}$.

So far, the clue is clear for us to design a dielectric material with a high energy-storage density, that is the material should have a high dielectric constant and a high dielectric strength (breakdown field) which allows the material to apply higher electric field. However, most of materials do not possess both these two properties at same time. Table 1.2 exhibits dielectric constant and dielectric strength of some common materials and it shows inorganic materials usually have higher dielectric constant but low breakdown field, inversely, organic materials have high breakdown field with low dielectric constant. Therefore, many current researches are focusing on the design of ceramic-polymer composite in order to combine properties of organic and inorganic materials to achieve high energy-storage density materials.

1.5 Research objectives

PVDF has full name Poly (vinylidene fluoride), molecule formula as Figure 1.7 (a), which is a ferroelectric polymer and has wide applications in electrical industry due to its excellent electrical property, high mechanical strength, good flexibility, great chemical stability and low process temperature. Although the ferroelectric property endows PVDF high dielectric constant, its nearly rectangle shape of displacement-electric field (D-E) hysteresis loop result in high dielectric loss and high remnant polarization which means small discharged energy-storage density and low efficiency [14] [15].

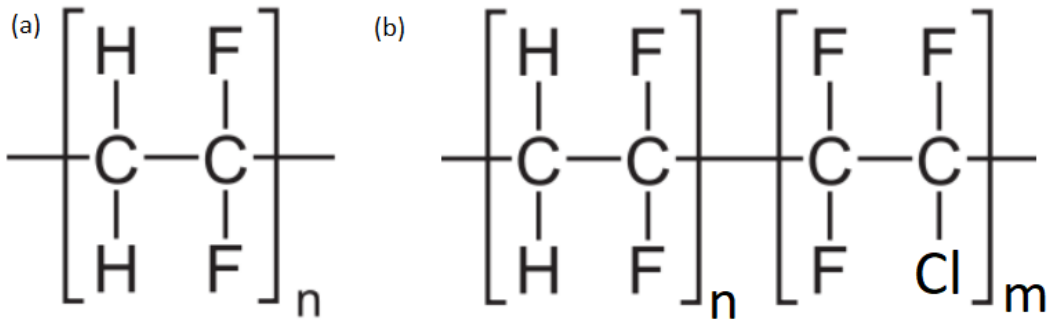

Figure 1. 7 Molecule formula of (a) PVDF and (b) P(VDF-CTFE)

Therefore, PVDF based copolymers are a better choice because the crystallinity and polar phase can be controlled through comonomer ratio [15]. P(VDF-CTFE) as Figure 1.7 (b) is a type of PVDF based copolymer, which has weak ferroelectricity and no clear phase transition at normal operating temperature range. Also, it is weakly temperature dependent on dielectric constant above its glass transition temperature and has better flexibility and lower crystallinity than that of PVDF [16] [17].

Recently, some papers report that PVDF and PVDF based copolymers blend with poly (methyl methacrylate) (PMMA) in order to decrease dielectric loss and increase energy efficiency, because PMMA is non-polar (weakly polar) material with low dielectric constant and loss, high dielectric strength and almost linear shape of P-E loops. The addition of PMMA can reduce the crystal size and crystallinity of PVDF and PVDF based copolymers, which enhances energy-storage density and minimize energy loss by reducing relaxation time of the composites at same time [16].

In this study, PMMA will be mixing into P(VDF-CTFE) to explore the dielectric properties of an ultrathin dielectric film fabricated by spin-coating process. The dielectric constant and dielectric loss will be measured at room temperature and different temperature, respectively. Polarization-electric field hysteresis loop and dielectric strength are tested to evaluate the ability of energy storage. Also, DSC is used to analyze phase transition of PMMA/P(VDF-CTFE) with different ratio of composition in order to have a better understanding of dielectric behaviors of the material.

CHAPTER 2

MATERIALS PREPARATION AND CHARACTERIZATION METHODS

2.1 Introduction

In this chapter, the fabrication process of PMMA-P(VDF-CTFE) films will be introduced. The improvement of our processing will be discussed comparing with traditional methods. Characterization methods also will be addressed in detail, such as measurement of dielectric constant, polarization-electric field and DSC test.

2.2 Preparation of PMMA-P(VDF-CTFE) films

2.2.1 Materials

PMMA-P(VDF-CTFE) films were fabricated by blending commercially available materials. P(VDF-CTFE) copolymer, has comonomer ratio of 91/9 mol %, named as VC91, its density is 1.75 g/cm^3, bought from Solvay. PMMA purchased from Fisher Scientific and its molecular weight is 35000 with density 1.18 g/cm^3. N, N-Dimethylformamide (DMF) as solvent bought from Fisher Scientific.

2.2.2 Spin-coating fabrication

One of improvement of this study is that spin-coating process is used rather than traditional solution casting process. The fabrication with solution casting process can prepare all-polymer or ceramic-polymer composite films with thickness of

dozens of microns and the film has critical disadvantages, such as poor uniformity in microstructure. Especially, fabrication of ceramic-polymer composite films has really bad quality because of the aggregation of ceramic particles and the gravity influence during the slow solidification. Therefore, many reports [7] [8] [11] use further process, such as hot press and chemical approaches, to improve the uniformity of composite films, however they are too complex. But, the process with spin-coating method has very simple steps, precise control and very excellent uniformity of ultrathin films because solidification is very fast due to the dispersion has less solvent [17].

2.2.3 Preparation process

The flowchart of fabrication process shown as Figure 2.1 and detailed steps are given following. First, PMMA and VC91 were weighed relied on Table 2.1 and mixed into 10 ml DMF in a 20 ml disposable scintillation vial with magnetic stirring. The mixture is dispersed by ultrasonic vibration (Ultrasonic Cleaners, Cole-Parmer Instrument company) for 1 h and magnetic stirring at 80℃ with 600 rpm for 1 h, alternately. The total dispersion is 10 h and, PMMA and VC91 were dissolved to be stable and uniform PMMA-VC91-DMF solution. A spin coater was operated to make films on glass substrate (Micro slides, 75×50 mm, Corning Incorporated) and was set as two steps, 1000 rpm for 10 s and 300 rpm for 15 s. The PMMA-VC91-DMF solution is about 1.5 ml that was dropped onto the center of a substrate. After coater stopped, samples should be moved into an oven immediately at 80℃ for 1 h. The solution layer was solidified very quickly due to the evaporation of DMF.

Table 2. 1 Volumetric ratios in PMMA-VC91

Vol. % of PMMA	VC91 (g)	PMMA (g)	DMF (ml)
0	1.5	0	10
1	1.5	0.01016	10
2	1.5	0.02052	10
3	1.5	0.0311	10
4	1.5	0.0419	10
5	1.5	0.05293	10
10	1.5	0.11174	10
15	1.5	0.17747	10
20	1.5	0.25142	10
25	1.5	0.33523	10
30	1.5	0.43101	10
35	1.5	0.54152	10
40	1.5	0.67045	10
50	1.2	0.80455	10
60	1	1.00568	10
70	0.8	1.25152	10
80	0.6	1.60909	10
90	0.3	1.81023	10
100	0	2	10

Then, the film can be peeled off in deionized water. Samples with large volume percentage of PMMA are slight difficult to peel because they are very brittle. Next, films were annealed at 140℃ for 24 h in air. The thickness of films with different volume fraction of PMMA is all about 8 microns. Finally, a gold sputter (PELCO SC-6) was used to make electrodes on the two sides of each film with 3 mm diameter. These gold coated films were tested by following methods to characterize their properties.

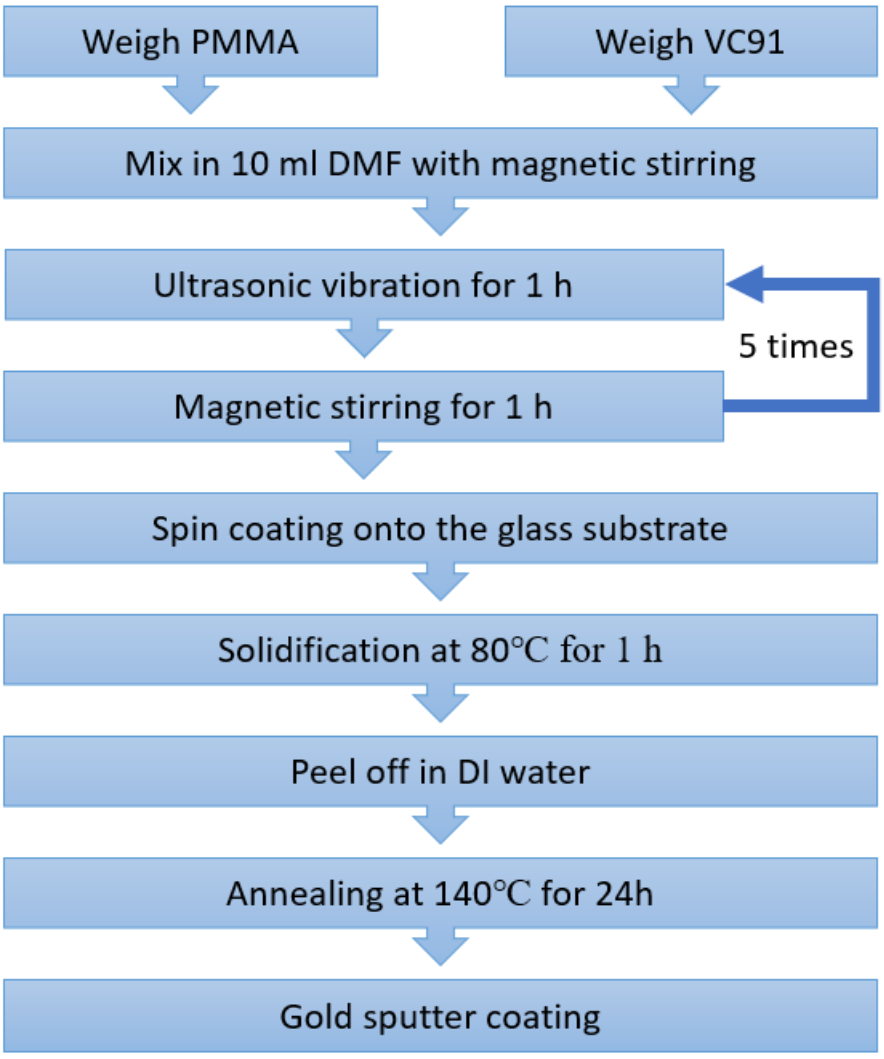

Figure 2. 1 Flowchart of fabrication process

2.3 Characterization methods

An impedance analyzer (Agilent 4294A precision) was used to measure dielectric properties of samples with frequency from 100 Hz to 1M Hz. The number of points for sweeping, adapter, measurement and source are set as 801, 1 M, Cp-D, 500 mV/div, respectively. Before starting tests, the impedance analyzer should be corrected under open and short conditions. Capacitance (C) and dielectric loss ($tan\delta$) were obtained by analyzer, equation (1.2) was used to calculate dielectric constant (ε_r') from capacitance. In this study, dielectric constant and dielectric loss were measured both at room temperature and in a range from -60℃ to 120℃, respectively. The dielectric properties with temperature dependence from -60℃ to 120℃, were measured at a temperature chamber (Espec ECT-2).

The polarization-electric field (P-E) hysteresis loops were tested by a Radiant Precision LC 100 system and a 10kV high voltage supply/Amplifier at 100 Hz in silicone oil. Software Vision is used to operate the device and can plot P-E loops directly. The energy-storage density can be obtained by calculation of area as Figure 1.6. Due to equation (1.5) and (1.6), electric displacement $\vec{D}$ and polarization $\vec{P}$ have approximately same value for a dielectric material which has dielectric constant much larger than 1. Therefore, P-E loops can be directly used to calculate energy-storage density (U).

Differential Scanning Calorimeter (DSC) was also used to test thermal response of PMMA-VC91 blends. The model of machine is Discovery series DSC250 bought from TA instrument, Inc. with a refrigerated cooling system of model number 90. Each sample was weighed about 10 mg and put into a Tzero aluminum

pan sealed by a Tzero press. An empty and same type pan was also tested at same time with the sample to measure the heat flow of samples when temperature was changing. The test was set starting from -90℃ and then temperature was increased with rate of 10℃ per minute until the temperature reached 250℃. After 1 minute maintaining 250℃, temperature was decreased with rate of 10℃ per minute. The test was ended after the temperature cooling to -90℃. The double circles test also was tested for pure VC91 by repeating above steps. The results of test will be discussed in next chapter.

CHAPTER 3

STUDY OF PMMA-P(VDF-CTFE) BLENDS

3.1 Study of dielectric properties at room temperature

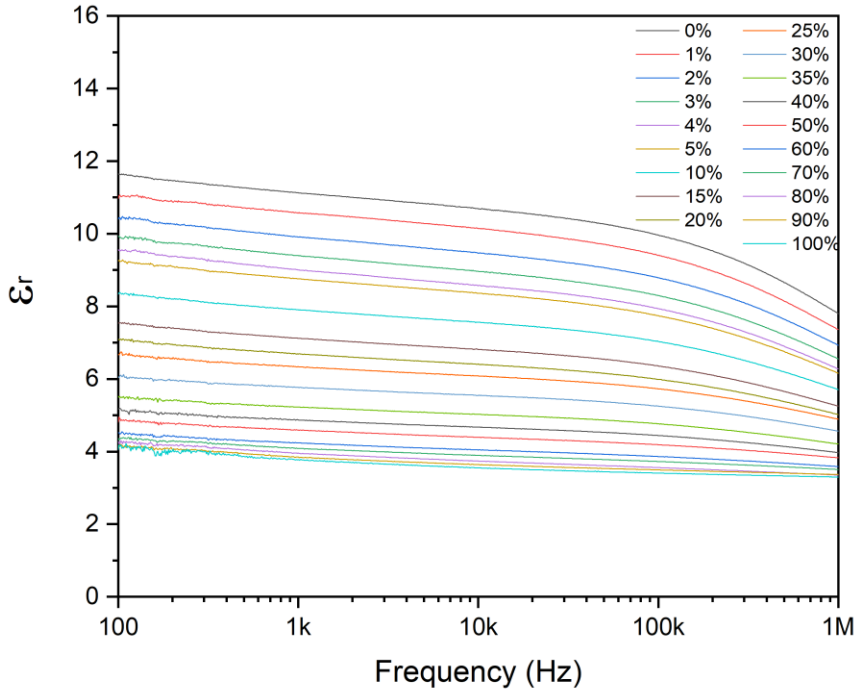

Figure 3.1. 1 Dielectric constant as a function of frequency at room temperature for PMMA-VC91 with 0 to 100 % of PMMA

The real part of relative permittivity or dielectric constant of PMMA-VC91 blends, which is shown in Figure 3.1.1 with the volume of PMMA from 0% to 100%, has dependence of frequency at room temperature. It is obvious that pure VC91 has strong frequency dependence and pure PMMA is weekly dependent of

frequency. Also, the frequency dependence of PMMA-VC91 blends is gradually decreased with the increase of volume of PMMA, which indicates that frequency dependence of the blends is mainly determined by VC91.

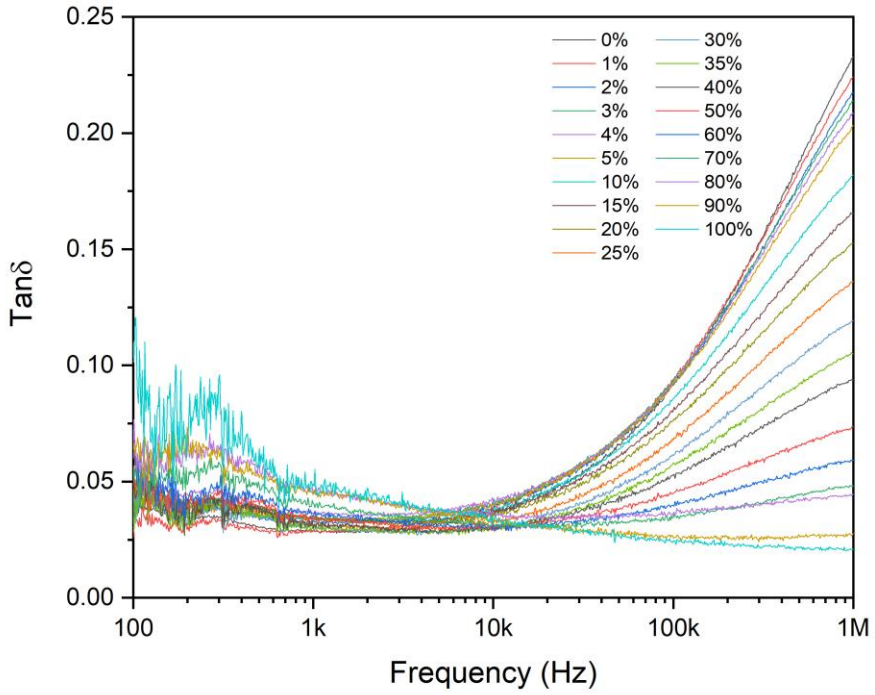

Figure 3.1. 2 Dielectric loss as a function of frequency at room temperature for PMMA-VC91 with 0 to 100 % of PMMA

The frequency dependence of dielectric loss at room temperature shown in Figure 3.1.2, will be discussed in PMMA-VC91 blends with different composition. The result shows dielectric loss (tanδ) is strongly dependent on frequency changes. In low frequency range, from 100 Hz to 10k Hz, tanδ is increased with increase of volume of PMMA. With high frequency range above 10K Hz, the tanδ is dramatically decreased with the increase of volume of PMMA. Apparently, PMMA

is slightly dependent of frequency due to the changes of tanδ from 0.1 (at 100 Hz) to 0.021 (at 1M Hz). But, pure VC91 has strong frequency dependence of tanδ from 0.033 (at 100 Hz) to 0.233 (at 1M Hz). It indicates that the tanδ of PMMA-VC91 is mainly determined by VC91.

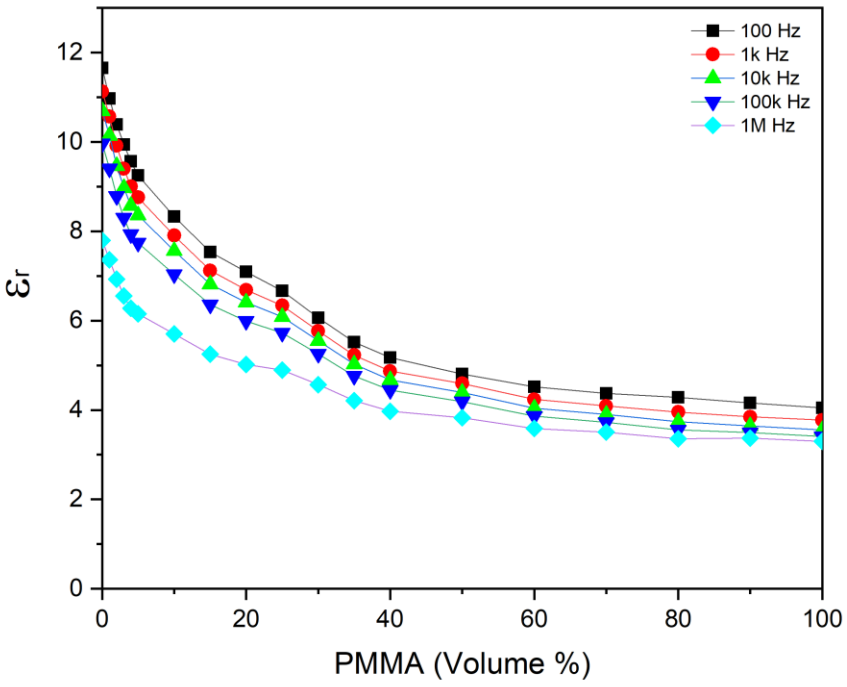

Figure 3.1. 3 Dielectric constant as a function of vol. % of PMMA at room temperature for PMMA-VC91 with 100 Hz to 1M Hz

The plot of the volume fraction influences on dielectric constant of PMMA-VC91 blends are shown in Figure 3.1.3. Obviously, dielectric constant steeply decreases with the increase of volume fraction of PMMA until 50%, but dielectric constant slightly decreases with the adding more PMMA above 50 vol. % of PMMA. First, the dilution effect of PMMA with relatively low dielectric constant

can be used to explain the behavior that the dielectric constant decreases with increase of volume fraction of PMMA. But this explanation cannot explain why the slopes are changed below 50% volume fraction of PMMA and the slope almost did not change above 50 vol. % of PMMA. The possible reason may have been that the crystallinity of blends decreases as the PMMA content increased, because crystallinity is also a factor to influence the dielectric constant at room temperature. Below 50 vol. % of PMMA, the crystallinity of blends decreases with increase of PMMA content. So, the slope of dielectric constant gradually decreases. Above 50 vol. % of PMMA, the slope of dielectric constant is almost constant, because crystallinity reaches minimum (about zero) at 50 % of PMMA and the blends above 50% of PMMA may be amorphous so that the dielectric constant decreases almost linearly. In conclusion, when the PMMA content is lower than 50 vol. %, the change of dielectric constant is mainly determined by crystallinity, but it is determined by dilution effect above 50 vol. % of PMMA. Therefore, the dielectric constant of PMMA-VC91 at room temperature and certain frequency is affected by both crystallinity of blends and composition. It is worth mentioning that dispersion between 100 Hz and 1M Hz gradually decreased as increase of PMMA content, which has difference about 4 at 0% of PMMA to about 0.7 at 100% of PMMA. The behavior was because the glass transition temperature of VC91 is below room temperature but that of PMMA is above room temperature, so that dielectric constant and loss of VC91 were dependent on frequency due to relaxation of motion of polymer chains but PMMA is not or slightly dependent on frequency because of frozen main chains.

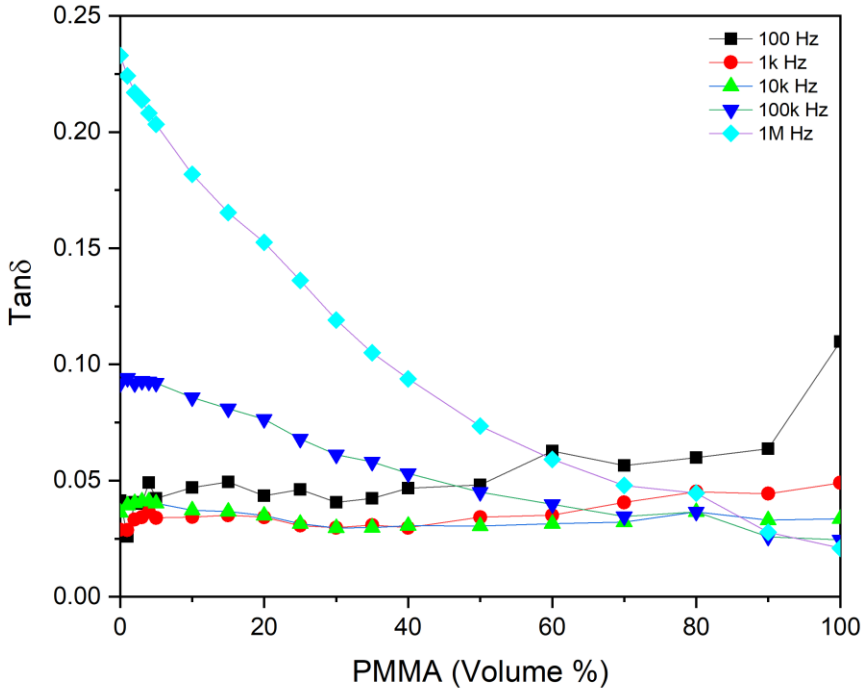

Figure 3.1. 4 Dielectric constant as a function of vol. % of PMMA at room temperature for PMMA-VC91 with 100 Hz to 1M Hz

The further plot of tanδ is shown in Figure 3.1.4 as function of volume fraction of PMMA. The dielectric loss of PMMA-VC91 blends remains very low, about 0.05, at low frequency range from 100 Hz to 10k Hz. While dielectric loss gradually decreases as the increase of PMMA content due to composition changes at high frequency. The dispersion of loss at 100 Hz and 1 M Hz also can be used same explanation as dielectric constant.

3.2 Study of temperature dependence of dielectric properties

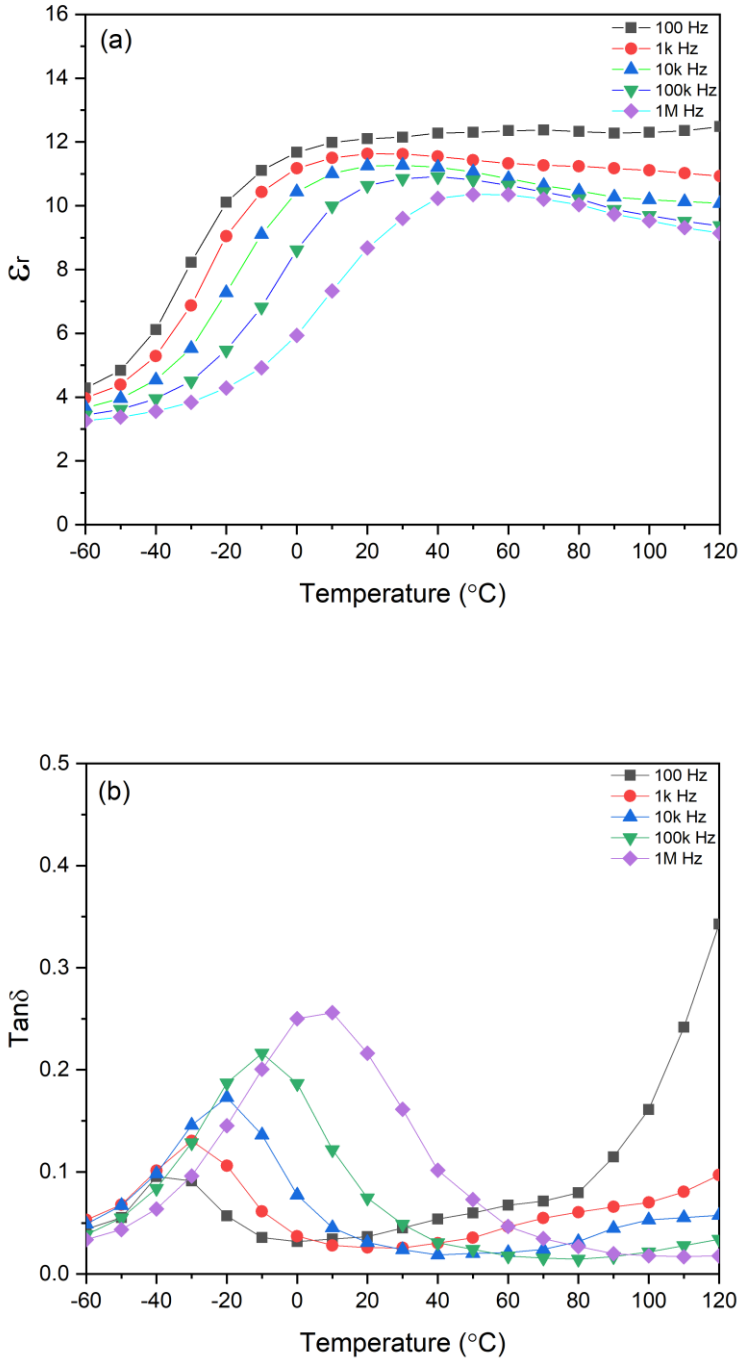

Figure 3.2. 1 Temperature dependence of dielectric constant (a) and dielectric loss (b) of pure VC91

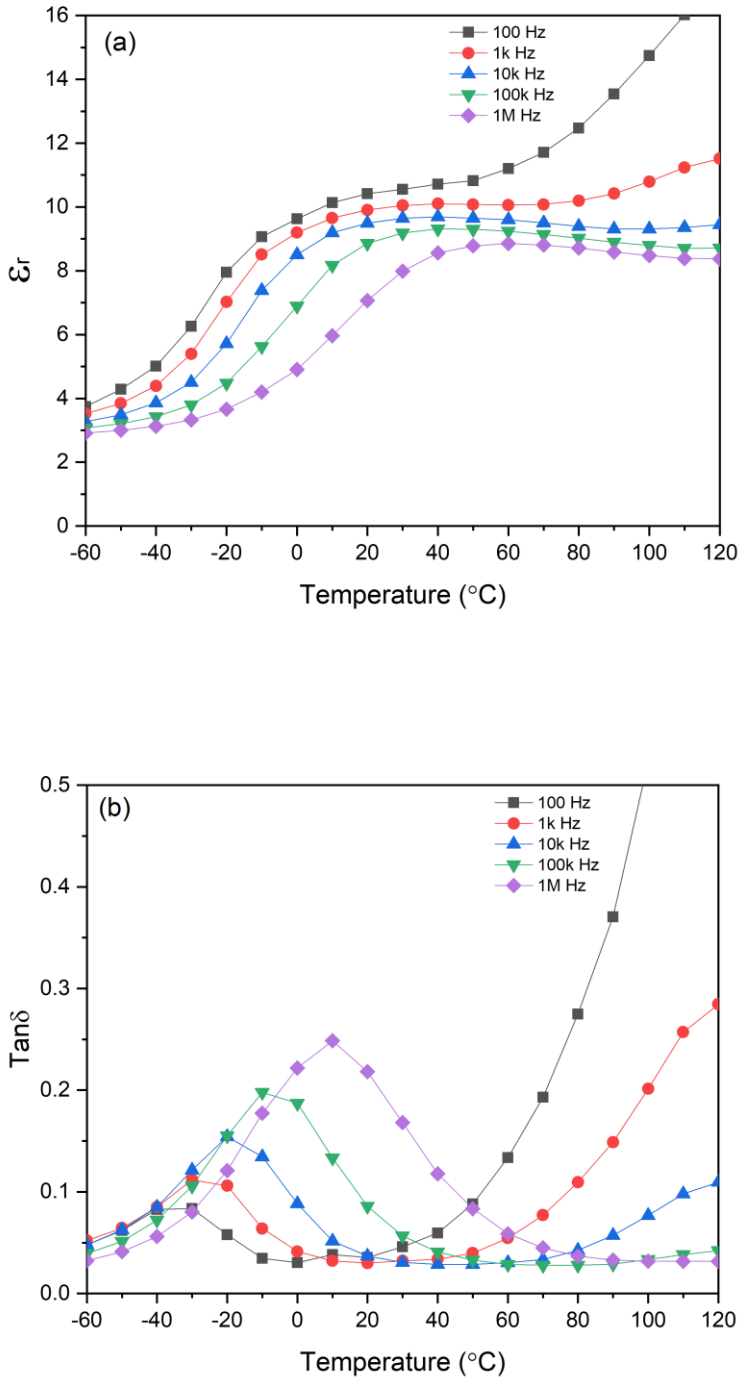

Figure 3.2. 2 Temperature dependence of dielectric constant (a) and dielectric loss (b) with 2% of PMMA

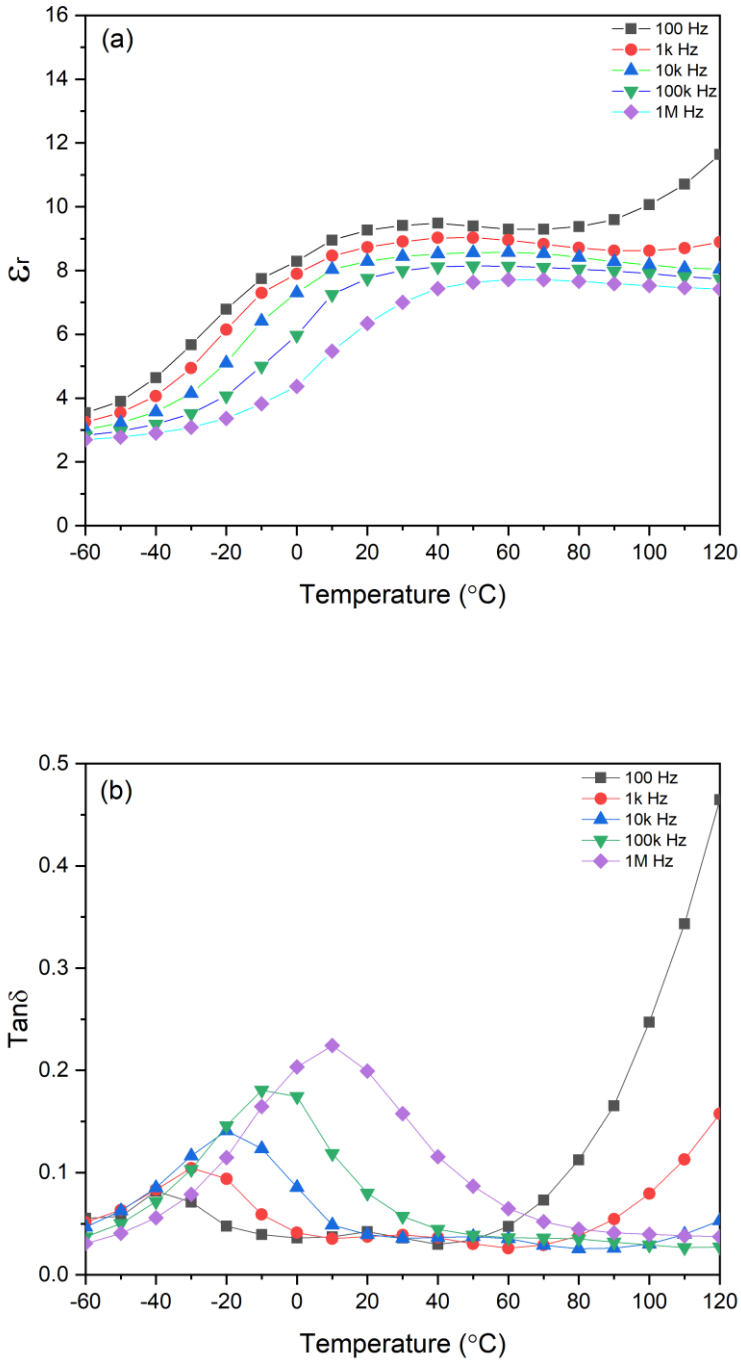

Figure 3.2. 3 Temperature dependence of dielectric constant (a) and dielectric loss (b) with 5% of PMMA

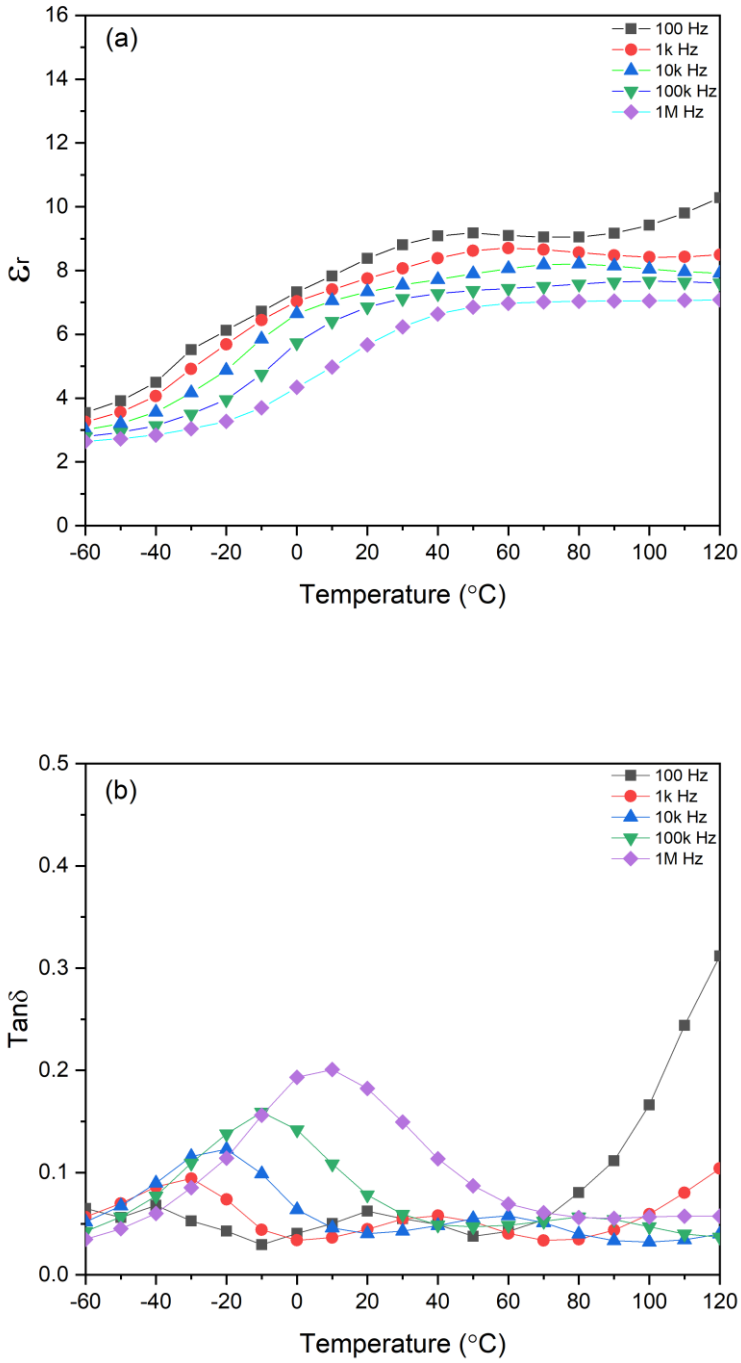

Figure 3.2. 4 Temperature dependence of dielectric constant (a) and dielectric loss (b) with 10% of PMMA

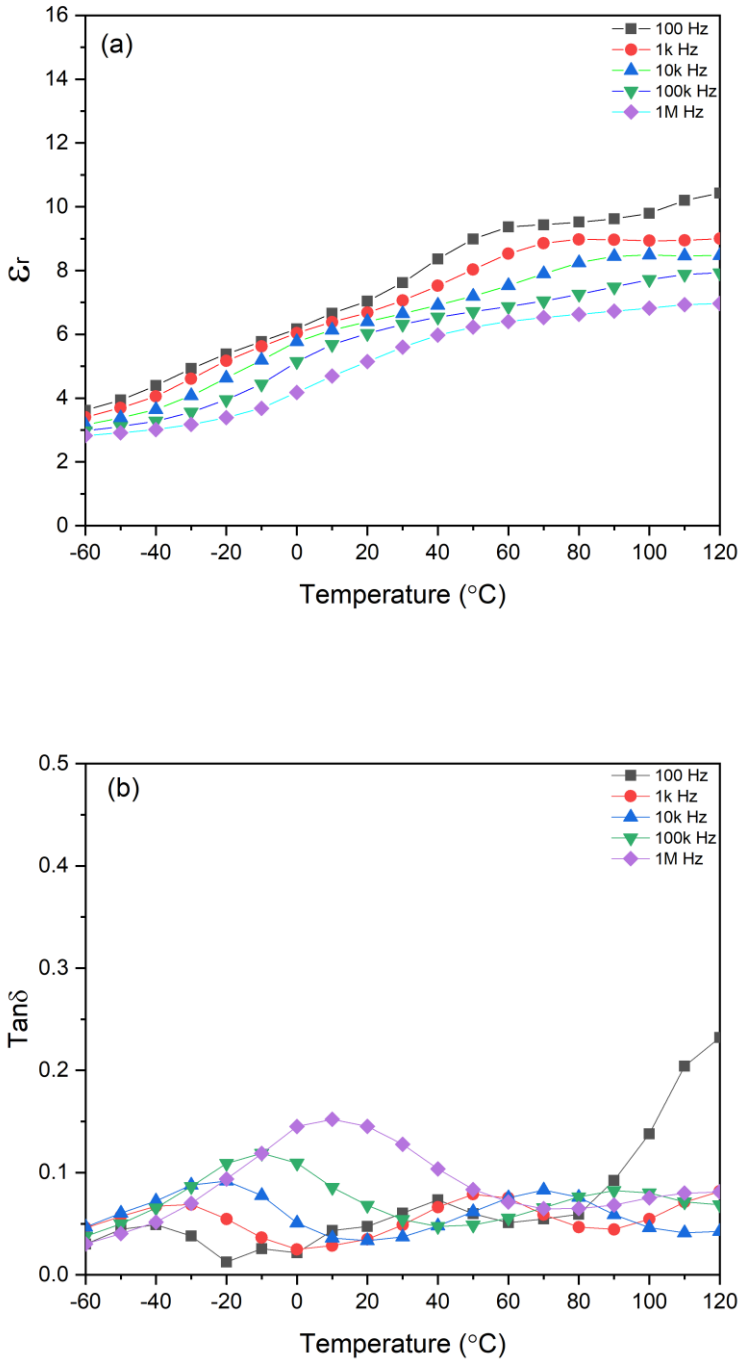

Figure 3.2. 5 Temperature dependence of dielectric constant (a) and dielectric loss (b) with 20% of PMMA

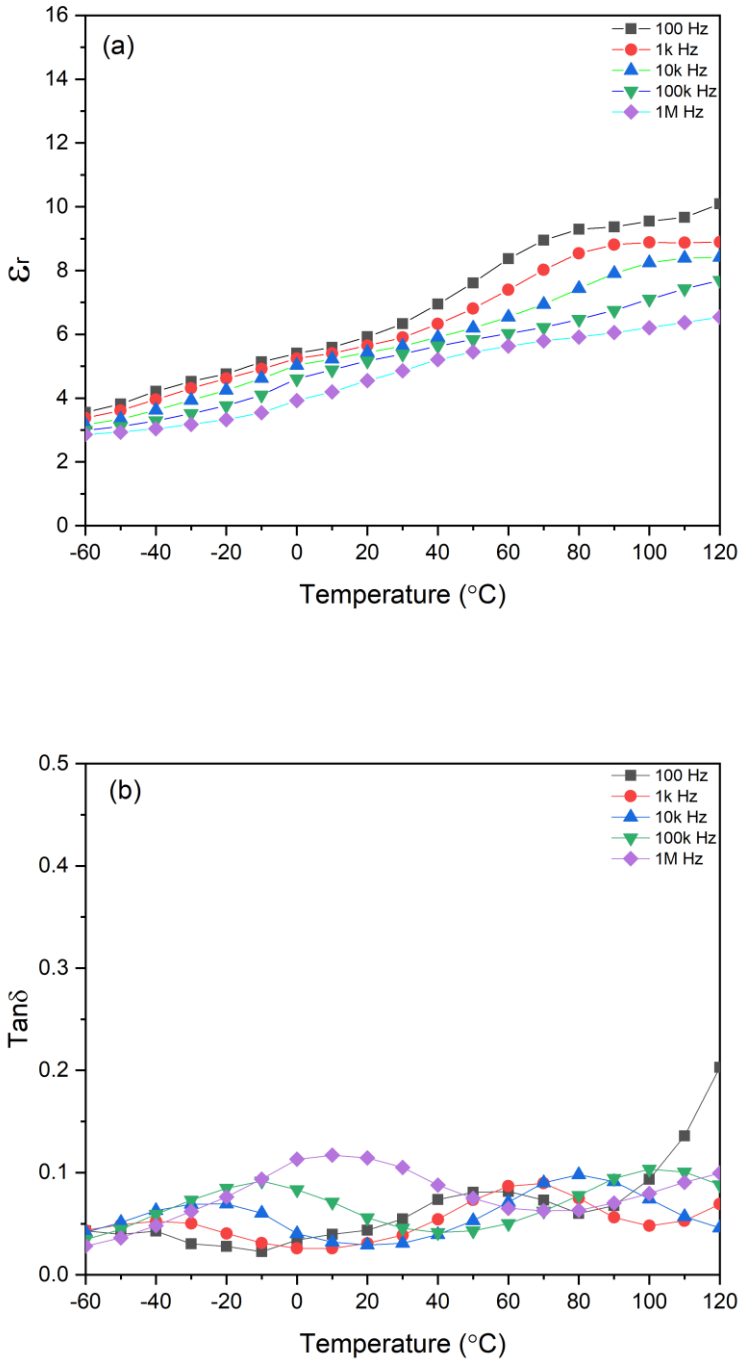

Figure 3.2. 6 Temperature dependence of dielectric constant (a) and dielectric loss (b) with 30% of PMMA

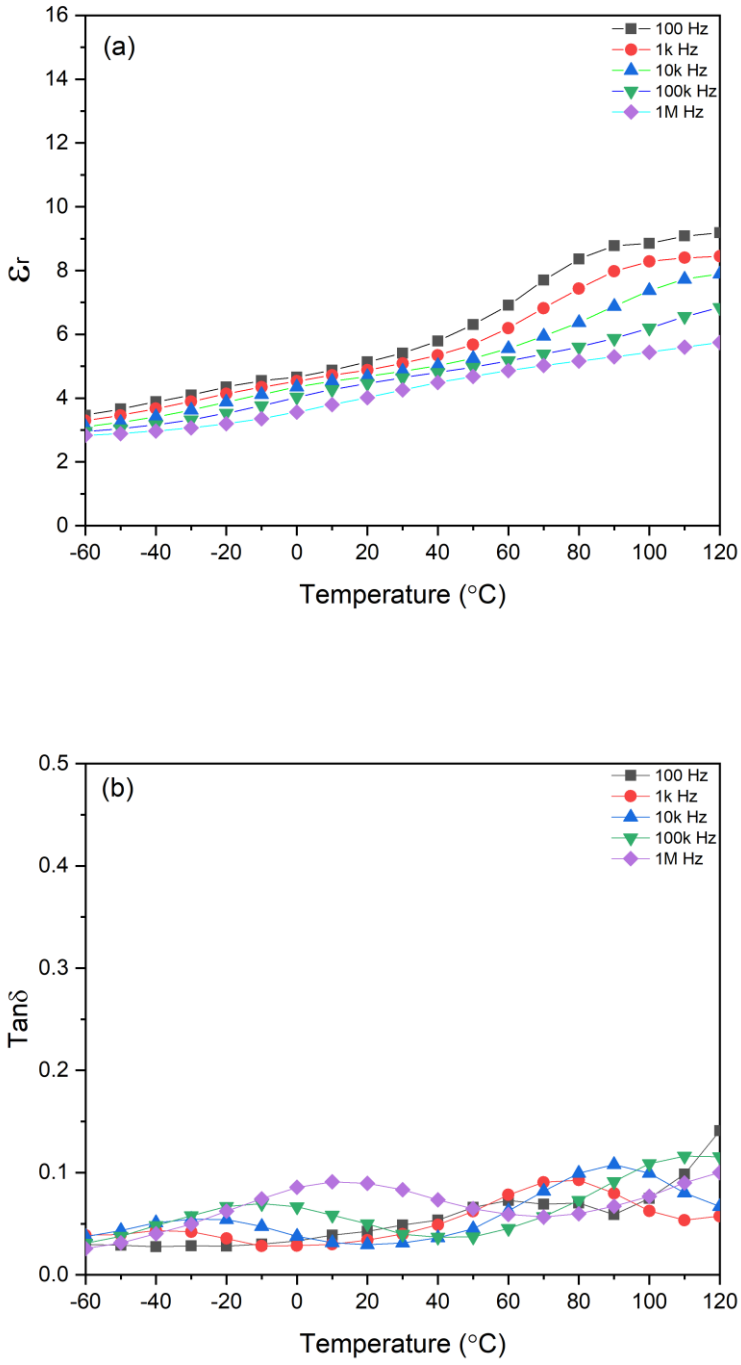

Figure 3.2. 7 Temperature dependence of dielectric constant (a) and dielectric loss (b) with 40% of PMMA

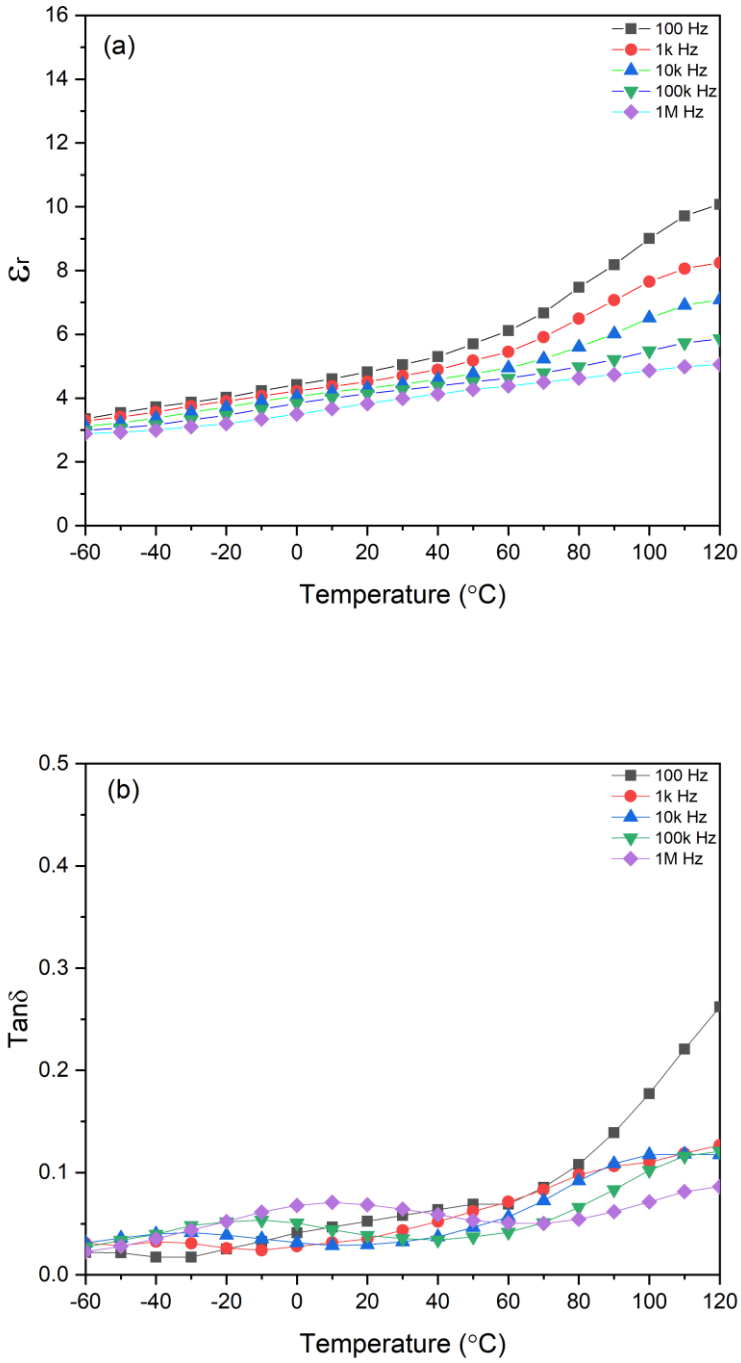

Figure 3.2. 8 Temperature dependence of dielectric constant (a) and dielectric loss (b) with 50% of PMMA

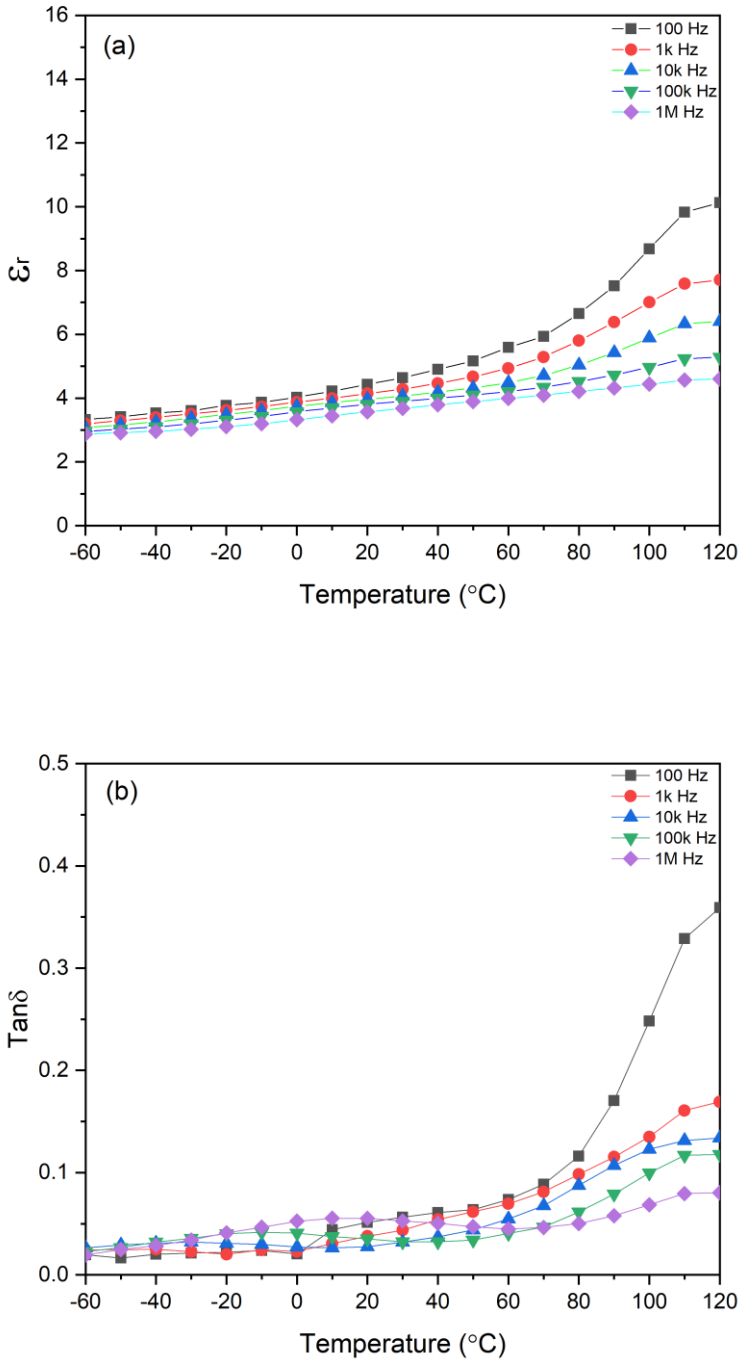

Figure 3.2. 9 Temperature dependence of dielectric constant (a) and dielectric loss (b) with 60% of PMMA

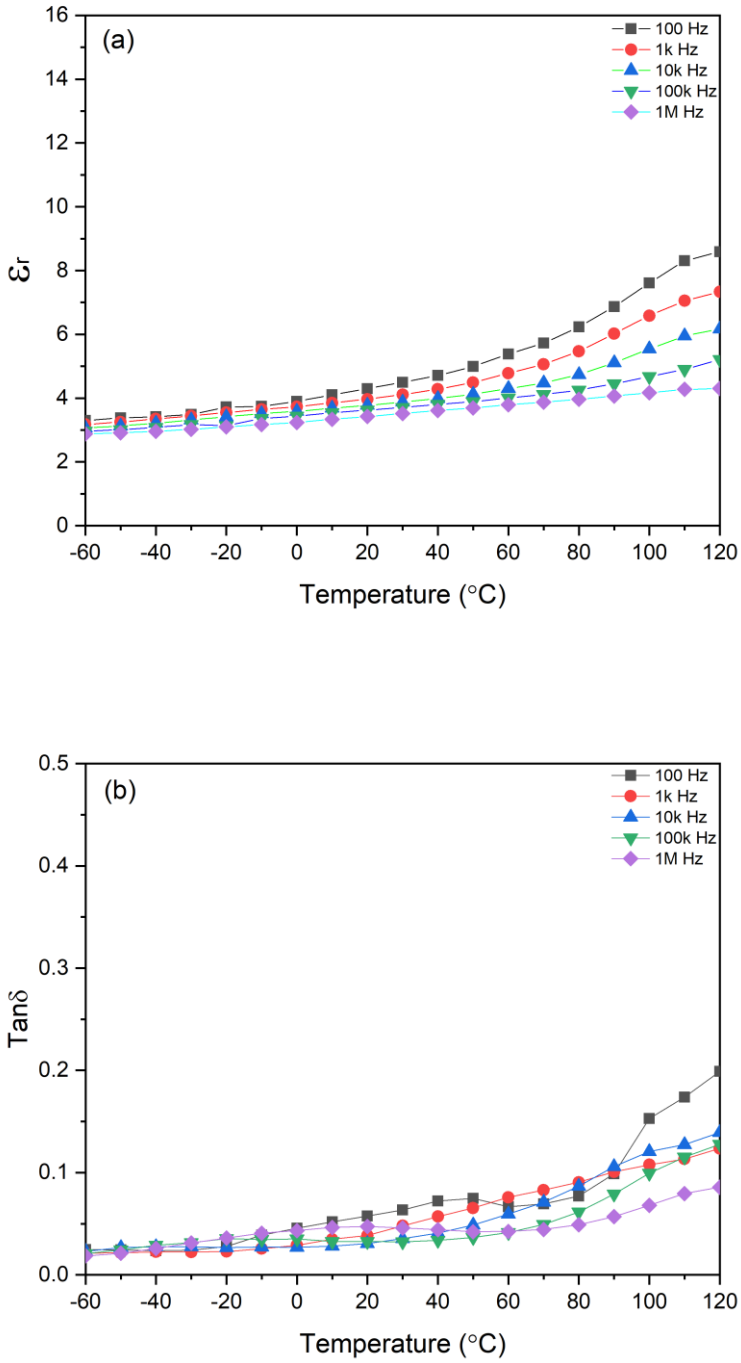

Figure 3.2. 10 Temperature dependence of dielectric constant (a) and dielectric loss (b) with 70% of PMMA

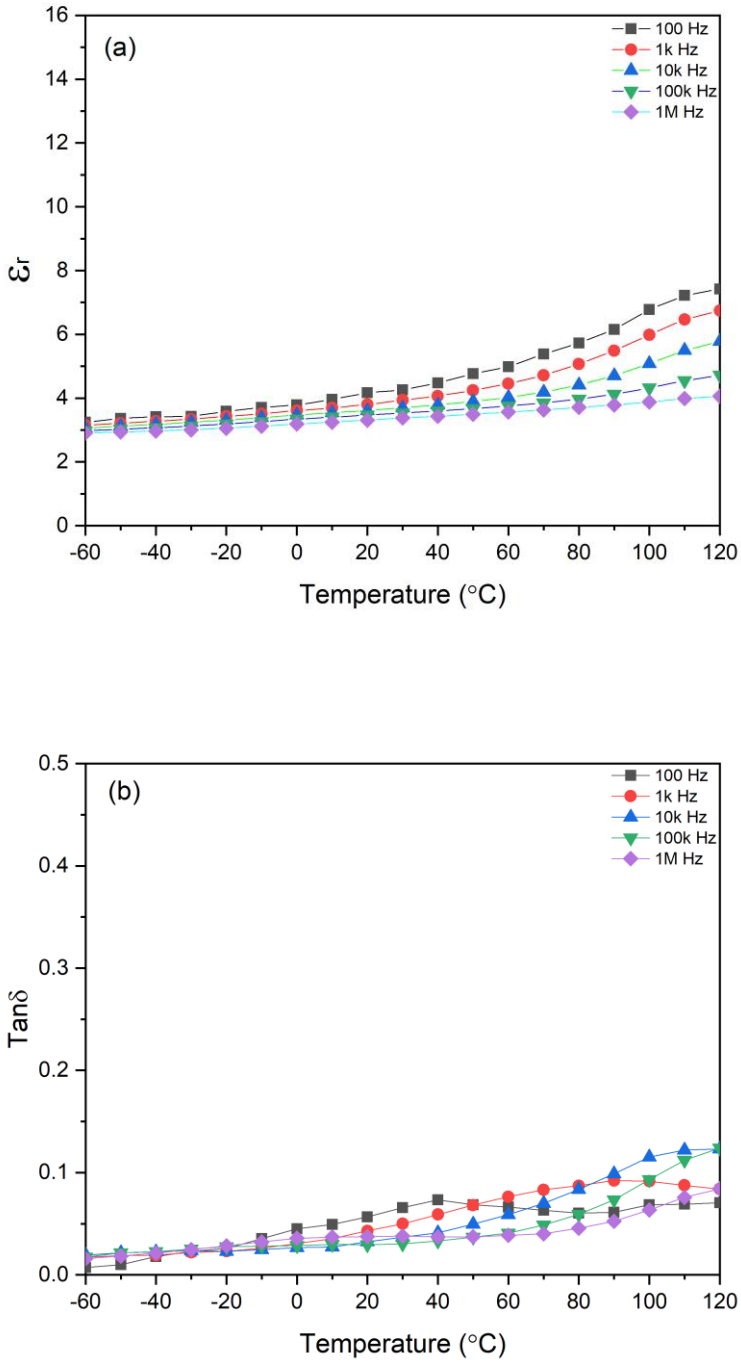

Figure 3.2. 11 Temperature dependence of dielectric constant (a) and dielectric loss (b) with 80% of PMMA

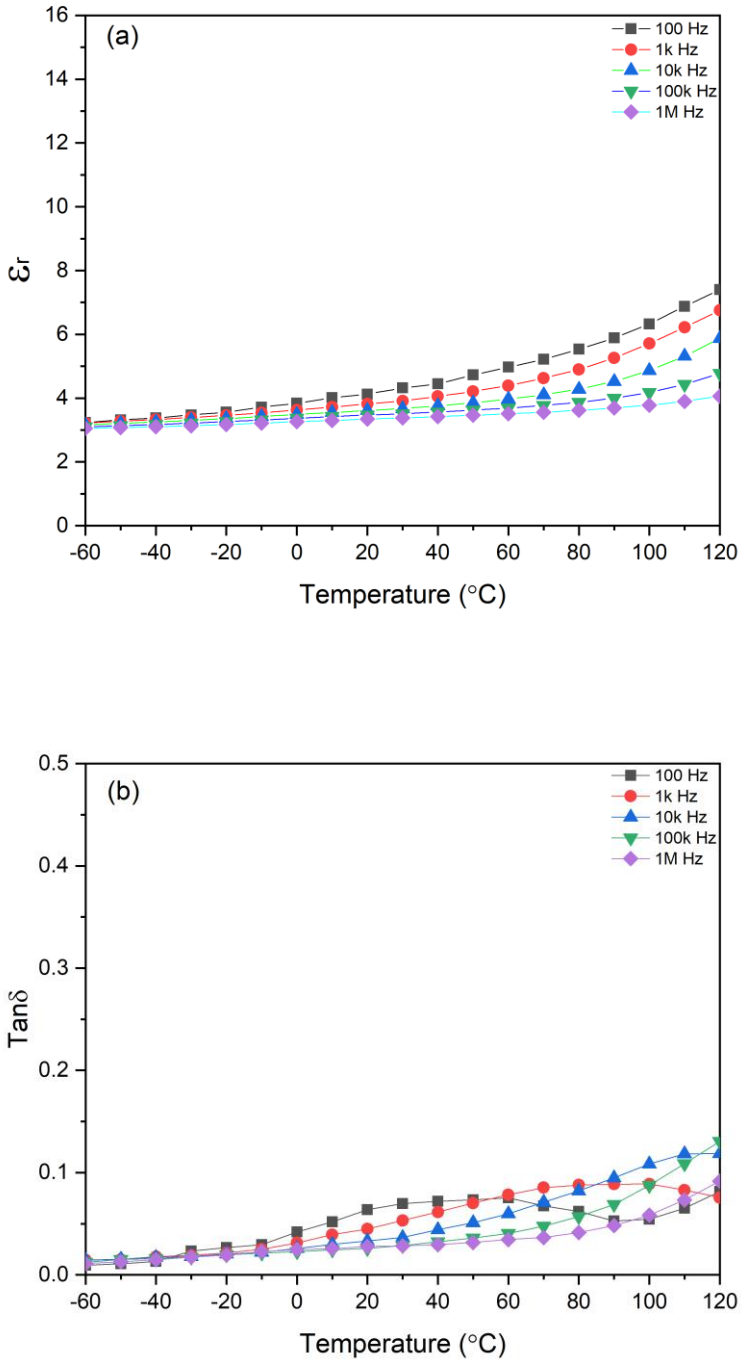

Figure 3.2. 12 Temperature dependence of dielectric constant (a) and dielectric loss (b) with 90% of PMMA

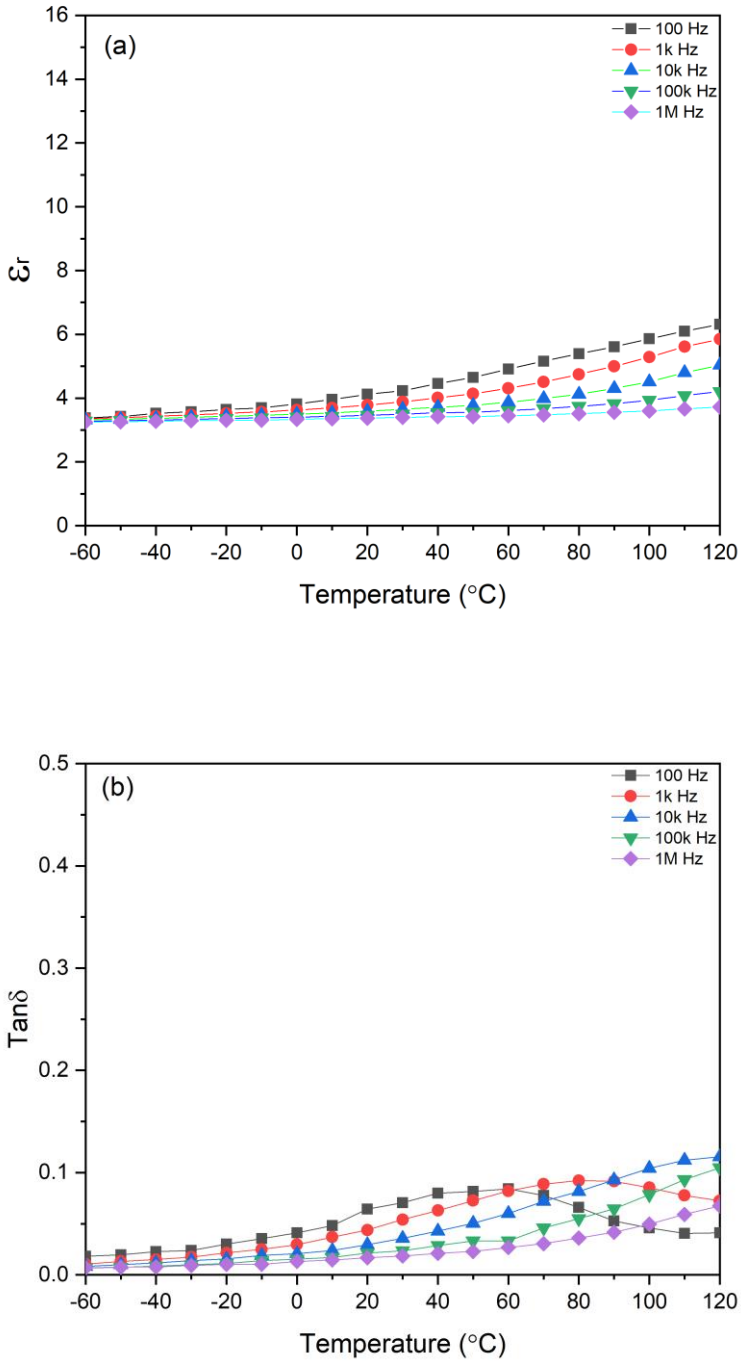

Figure 3.2. 13 Temperature dependence of dielectric constant (a) and dielectric loss (b) of pure PMMA

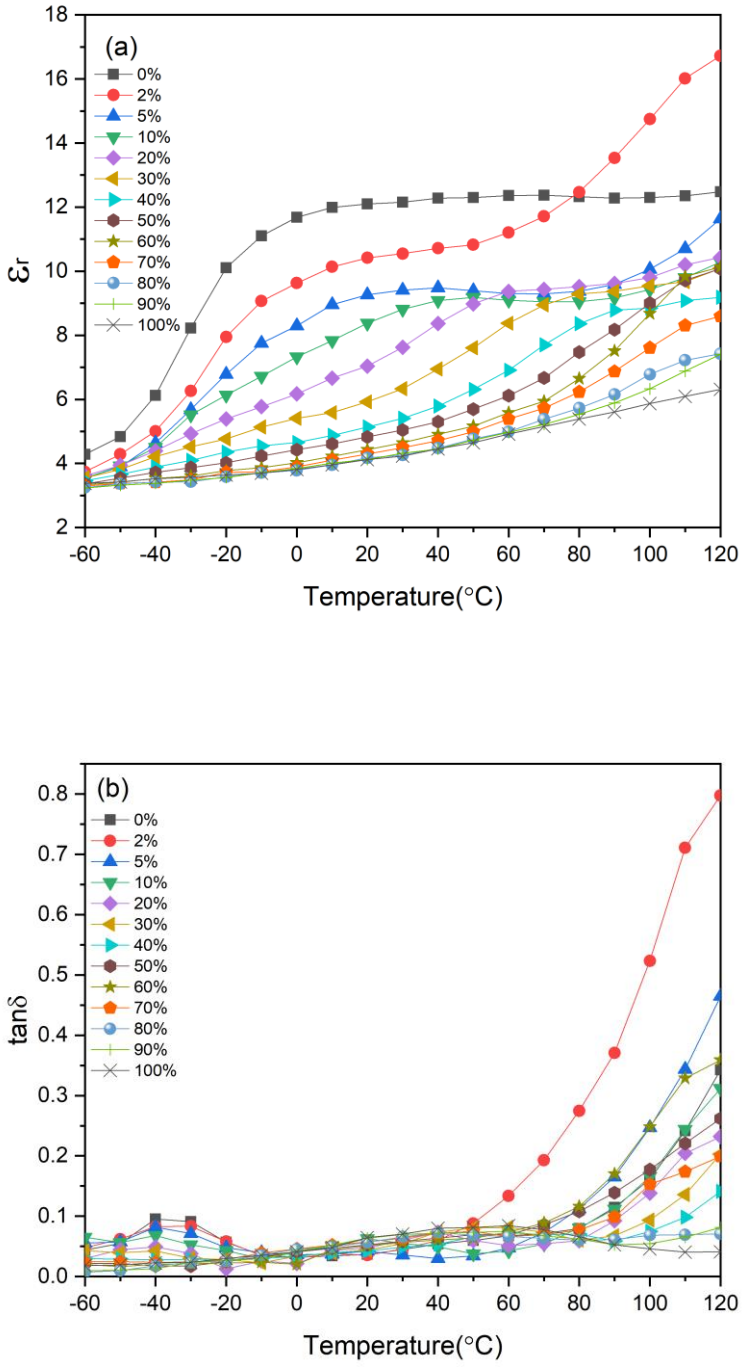

Figure 3.2. 14 Dielectric constant (a) and loss (b) of PMMA-VC91 as function of temperature at 100 Hz with 0 to 100 % of PMMA

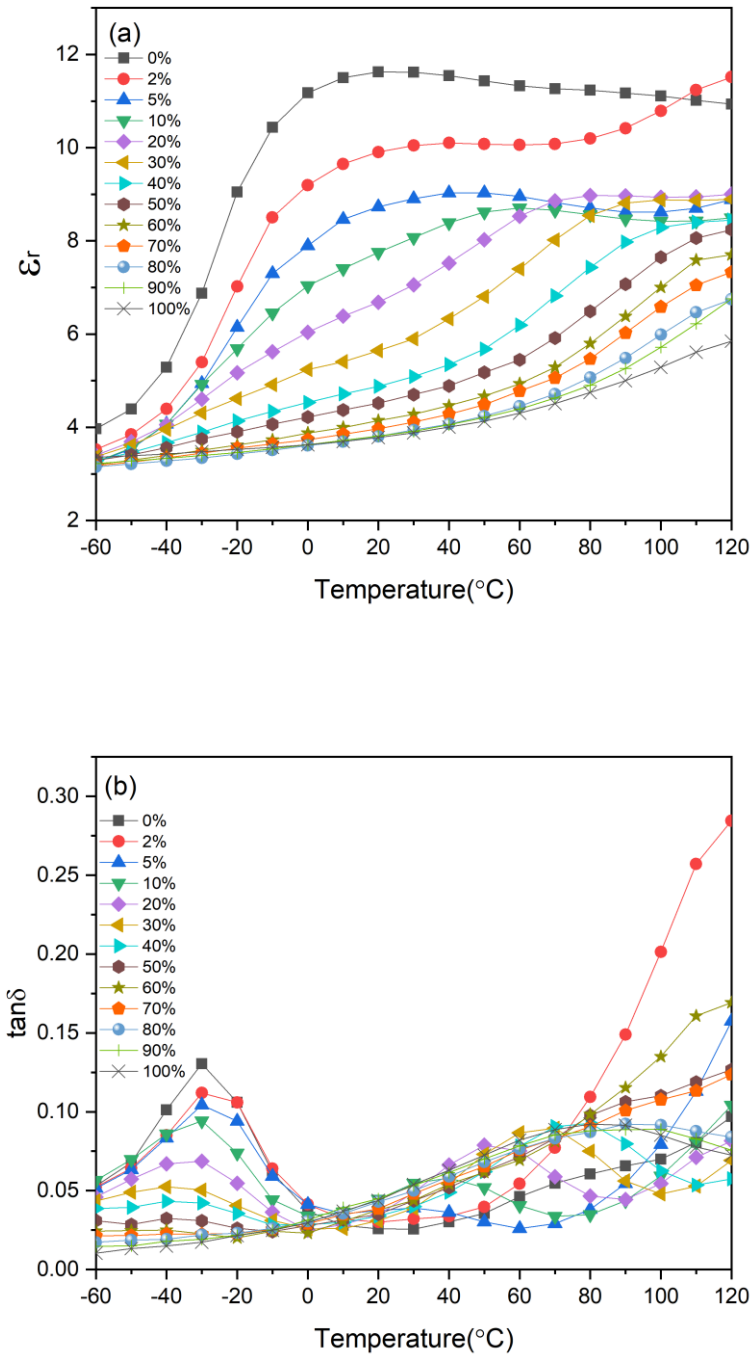

Figure 3.2. 15 Dielectric constant (a) and loss (b) of PMMA-VC91 as function of temperature at 1k Hz with 0 to 100 % of PMMA

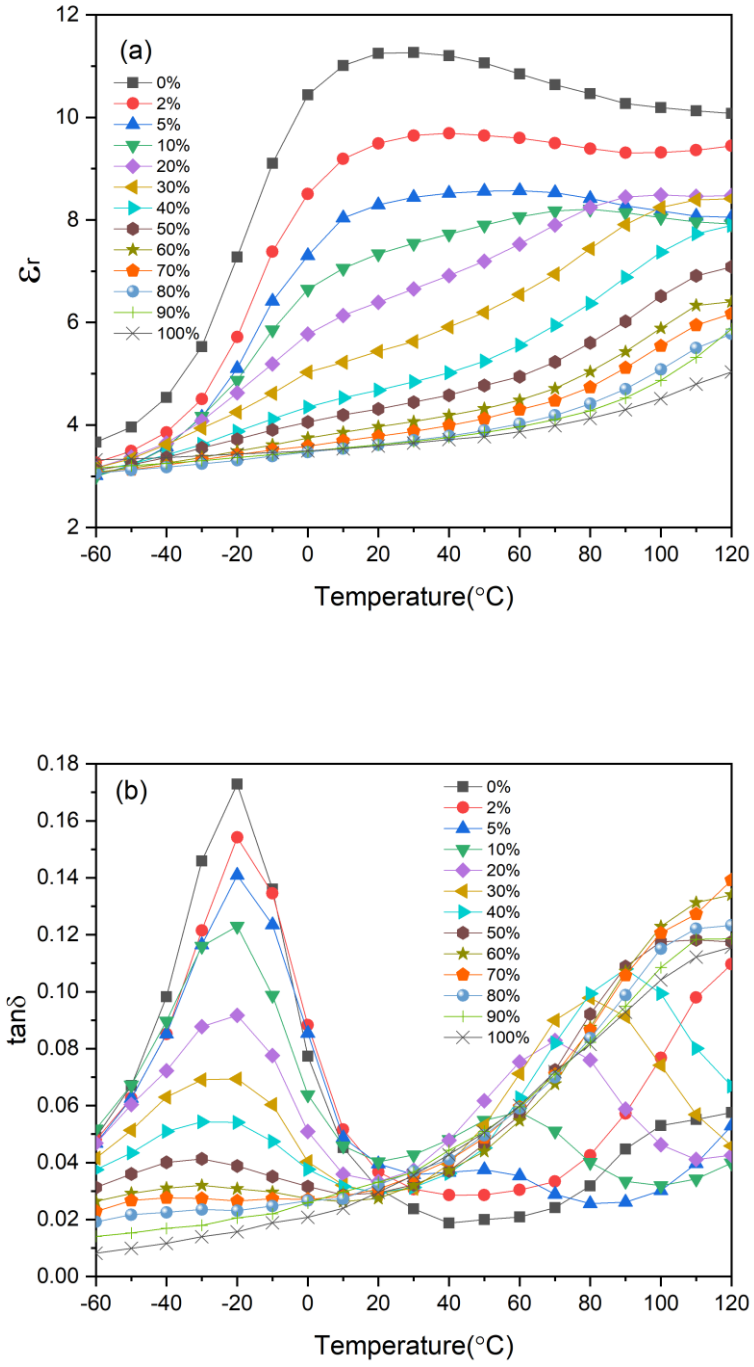

Figure 3.2. 16 Dielectric constant (a) and loss (b) of PMMA-VC91 as function of temperature at 10k Hz with 0 to 100 % of PMMA

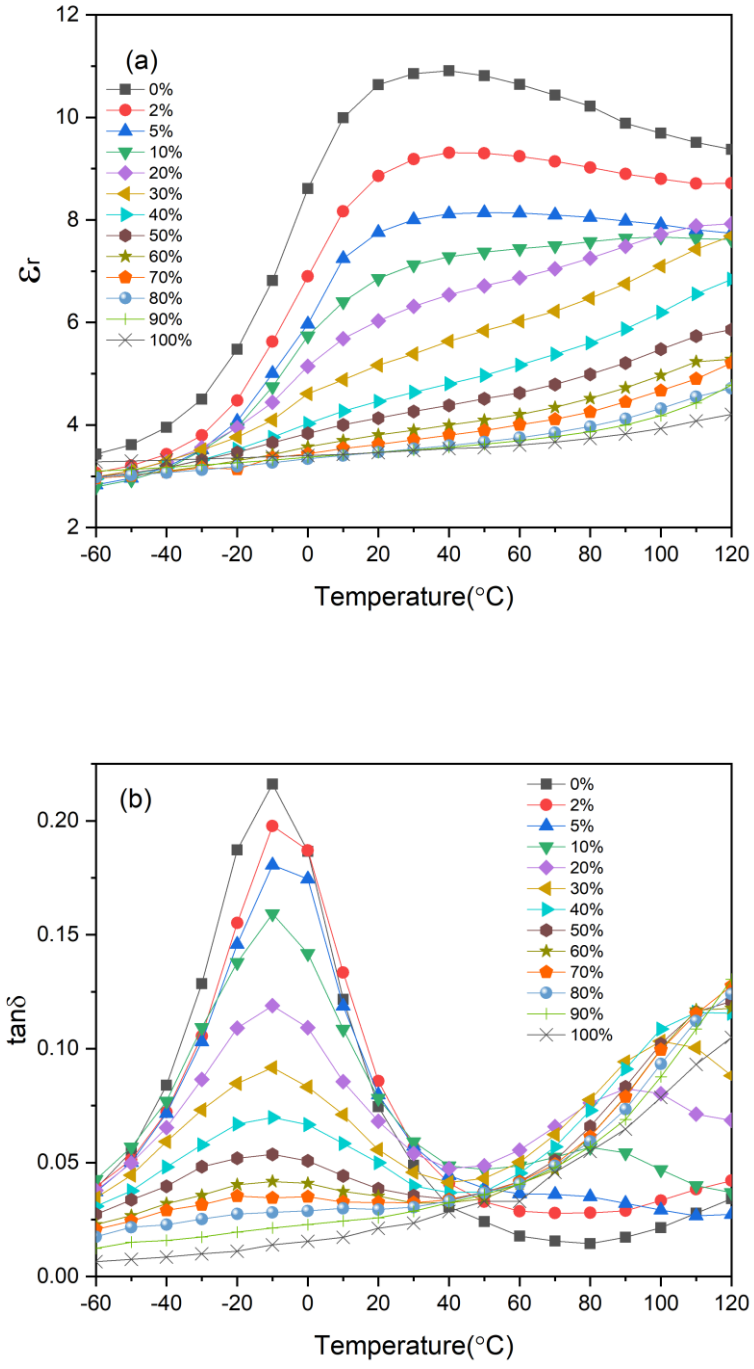

Figure 3.2. 17 Dielectric constant (a) and loss (b) of PMMA-VC91 as function of temperature at 100k Hz with 0 to 100 % of PMMA

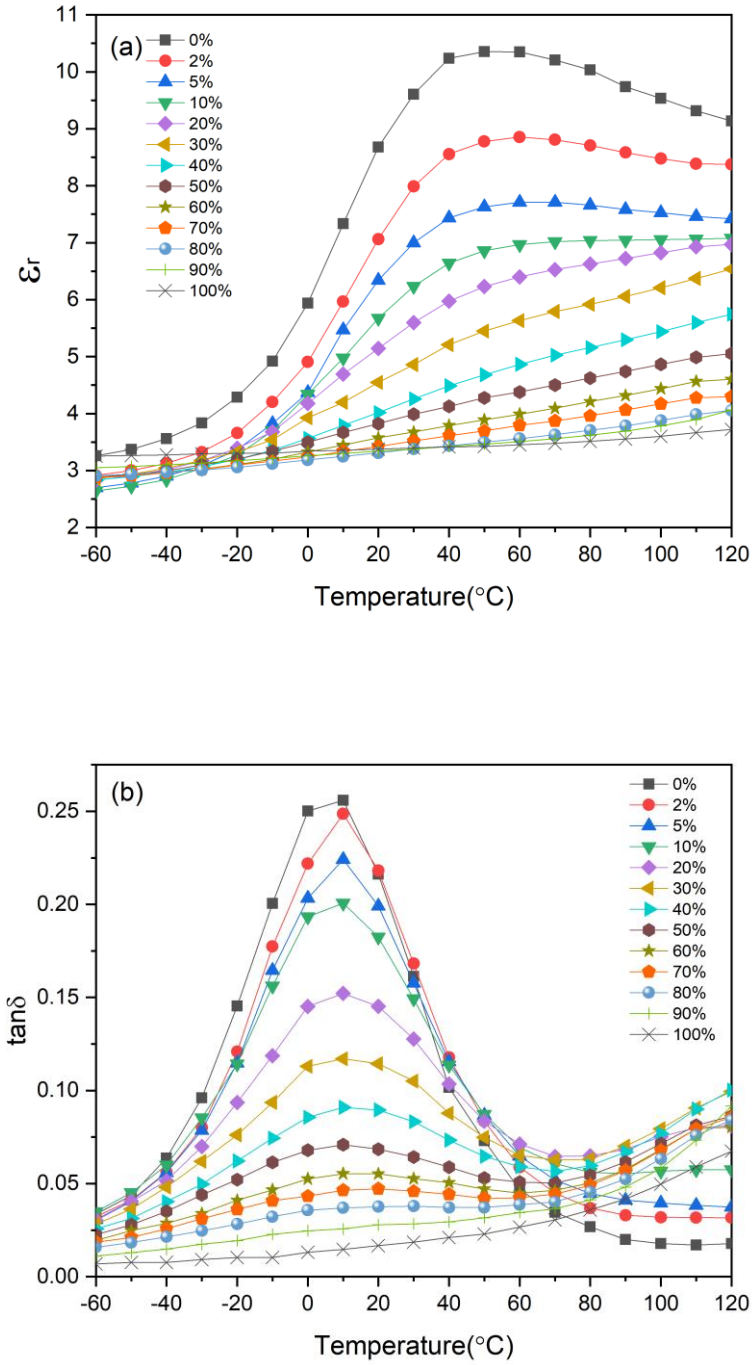

Figure 3.2. 18 Dielectric constant (a) and loss (b) of PMMA-VC91 as function of temperature at 1M Hz with 0 to 100 % of PMMA

The temperature dependences of dielectric constant and loss were characterized at several frequency of 100, 1k, 10k, 100k and 1M Hz, respectively. These dielectric properties with different volume fraction of PMMA, from 0% to 100%, were plotted in Figure 3.2.1 to 3.2.13, as function of temperature from -60℃ to 120℃ and it indicated that the dielectric constant and loss are dependent on temperature. Figure 3.2.1 and 3.2.13 show the dielectric constant and loss of pure VC91 and pure PMMA. For pure VC91, it has strongly dependence of temperature because dielectric constant at 100 Hz was changed from about 4 at -60℃ to about 12 at 120℃ and dielectric loss at 100 Hz was also increased from about 0.05 at -60℃ to about 0.35 at 120℃. But pure PMMA has relatively weaker temperature dependence than that of pure VC91 due to its small changes of dielectric constant and loss (range of ε_r and $\tan\delta$ is 3.3-6.3 and 0.006-0.115). Comparing plots from Figure 3.2.1 to 3.2.13, the dielectric constant and loss are gradually decreased as the increase of PMMA content because of the low dielectric constant and loss of PMMA due to its nonpolar material.

The discussion of properties of PMMA-VC91 blends will be separated to two parts, low temperature range (from -60℃ to around 30℃) and high temperature range (from around 30℃ to 120℃). In Figure 3.2.1 (a), the dielectric constant of pure VC91 is dramatically increased in low temperature range. The behavior was well-known by previous researches, the dramatic change of dielectric constant in low temperature range is attributed to relaxation process associated with glass transition of VC91 which has temperature about -40℃ [18]. Also, the dielectric loss in Figure 3.2.1 (b) has a series of peaks starting at about -40℃ in low

temperature range due to the same explanation that relaxation process associated with glass transition. As we discussed, the glass transition process of VC91 leads to dramatic changes of dielectric constant and peaks of dielectric loss in low temperature range. Figure 3.2.1 (a) and (b) exhibit several temperatures we named as the change temperature and peak temperature which express a temperature when the slopes of dielectric constant change and curves of dielectric loss reach the maximum value in low temperature range at each frequency, respectively, and these two temperatures seem to be same value. Apparently, for pure VC91, the change and peak temperatures increase with increase of frequency, and this result also shows in other PMMA-VC91 blends with low volume fraction of PMMA. It indicates glass transition temperature of VC91 increased with the increase of frequency. For pure PMMA in Figure 3.2.13, dielectric properties do not change too much because the glass transition temperature of PMMA is not in low temperature range. The glass transition temperature of PMMA is about 105℃ so that the relaxation process associated with glass transition of PMMA did not show clearly in blends below 120℃. The above dielectric behaviors in low temperature range, such as dramatically increased dielectric constant and peaks of dielectric loss, from Figure 3.2.1 to 3.2.8, were gradually decreased with increase of volume fraction of PMMA from 0% to 50%, because these behaviors were determined by VC91 which are reduced with the decrease of VC91 content. After greater than 50 vol. % of PMMA, above dielectric behaviors are almost disappeared or very weak in low temperature range, which can be explained that PMMA dominates dielectric properties.

The influence of composition change of PMMA-VC91 blends on temperature dependence was furtherly studied, the dielectric constant and loss were plotted as from Figure 3.2.14 to 3.2.18 at 100 Hz, 1k Hz, 10k Hz 100k Hz and 1M Hz, respectively. The relationship between dielectric constant and PMMA content is shown clearly that dielectric constant decreases with increase of PMMA content at temperature from -40℃ to 40℃, but it is complex in high temperature range and we will discuss later. It is worth mentioning that the dramatic change of dielectric constant due to glass transition relaxation process of VC91 became weaker with adding higher volume fraction of PMMA. The relaxation process associated with glass transition of VC91 almost disappeared after adding more than 50% of PMMA as we discussed previously. It indicated that the addition of PMMA can repress the relaxation process due to glass transition of VC91, because of the reduction of VC91. The dielectric loss with the influence of PMMA content at same frequency is shown in Figure (b) from 3.2.14 to 3.2.18. The peaks of dielectric loss due to relaxation process associated to glass transition process of VC91 was discussed before and the value of peaks gradually decreases with increase of PMMA content due to reduction of VC91. Also, the peaks were all at same temperature about -40℃, -30℃, -20℃, -10℃ and 10℃ at 100 Hz, 1k Hz, 10k Hz, 100k Hz and 1M Hz, respectively. The result is different with ceramic-polymer composite [19], which means PMMA did not change the glass transition of VC91.

In high temperature, the dielectric constant and loss shown in Figure 3.2.1 to 3.2.13, were roughly decreased with increase of PMMA constant due to the addition

of PMMA and low dielectric properties of PMMA. Obviously, the dielectric behaviors are very complicated, so it will be separated into three parts to discuss.

The first part is PMMA-VC91 blends with 0% to 40% of PMMA. The curve shape of dielectric constant and loss are similar because the dielectric behaviors are dominated by VC91 due to its higher volume fraction. The typical dielectric behavior of pure VC91 as Figure 3.2.1 (a) and (b) was well-known by previous studies [16] [17] [20]. It is reported that the increase of dispersion of dielectric constant and loss at low frequency in high temperature is contributed by relaxation process of motion of polymer chains in amorphous region of VC91. A special behavior appears at Figure 3.2.2 that the dispersion of dielectric constant and loss of the blend with 2% of PMMA at low frequency in high temperature obtained largest and values of dielectric constant and loss at 100 Hz got maximum, comparing with the blends with 0% and 5% of PMMA. It can be explained by decrease of crystallinity of VC91 after adding PMMA or fillers, this phenomenon was mentioned in literature [17]. The decrease of crystallinity can increase the motion of polymer chains of VC91 in high temperature, so that dielectric constant and loss at low frequency becomes larger due to stronger relaxation process. However, the dispersion of dielectric constant and loss at low frequency in high temperature gradually decreased with adding more PMMA until 40%, because the reduction of VC91 content and VC91 related dielectric properties become weaker. Therefore, the dispersion of dielectric constant and loss in high temperature decreased from 2% to 40% of PMMA.

Another behavior of dielectric constant in Figure 3.2.1(a), 3.2.2 (a), 3.2.3 (a), 3.2.4 (a), 3.2.5 (a), 3.2.6 (a) and 3.2.7(a) can be discovered easily that there are peaks moving to higher temperature from 0% to 40% of PMMA, especially at low frequency, such as 100 Hz and 1k Hz. It should use a new relaxation process to explain. As discussed previously, the glass transition of VC91 was shown in Figure 3.2.14 (b), 3.2.15 (b), 3.2.16 (b), 3.2.17 (b) and 3.2.18 (b), that glass transition temperature of VC91 did not change with the increase of PMMA content. And the glass transition of PMMA at 105℃ was not obvious in the test range from -60℃ to 120℃. Therefore, a new relaxation process must exist to contribution of this behavior. A series of peaks of dielectric loss in high temperature range were gradually moving to higher temperature and enhancing to greater value with increase of PMMA content, it is clear shown in Figure 3.2.16 (b). It indicates the new relaxation process really exists and related to change of composition. The possible reason is that the glass transition of PMMA-VC91 blends and glass transition temperature increased with increase of PMMA content. According to our polymer knowledge, VC91 has large molecular weight so that PMMA is hard to dissolve into VC91, but VC91 can dissolve into PMMA. Therefore, in the condition of low content of PMMA, there are probably two phases in samples, one is VC91 and another is PMMA-VC91 blend. The influence of VC91 in samples on dielectric properties was discussed previously, but the dielectric properties of PMMA-VC91 blend are not clear so far. The more PMMA content was added, the more VC91 dissolved in to PMMA. So, the glass transition temperature increased with increase of PMMA content, which can be explained by equation (3.1)

$$lnT_g = W_1 lnT_{g1} + W_2 lnT_{g2} \quad (3.1)$$

where T_g means glass transition temperature of blend, T_{g1} and T_{g2} represent the glass transition temperature of two polymers, W_1 and W_2 are weight fraction of two polymers [22]. The value of peak in high temperature increased with increase PMMA content in Figure 3.2.16, because relaxation process associated with the glass transition of blend enhanced with PMMA content. It indicates that relaxation process related to glass transition of PMMA-VC91 in high temperature was dominated by dielectric properties of PMMA. Now the movement of peaks of dielectric constant in Figure 3.2.1(a), 3.2.2 (a), 3.2.3 (a), 3.2.4 (a), 3.2.5 (a), 3.2.6 (a) and 3.2.7(a) is due to relaxation process of glass transition of PMMA-VC91 blend.

The second part is the behavior in Figure 3.2.8, 3.2.9 and 3.2.10 with 50% to 70% of PMMA in PMMA-VC91 blends. It is obvious that dielectric constant and loss in high temperature were increased at 50% and 60% of PMMA and then decreased with adding more PMMA. This behavior does not match with the rough trend of PMMA-VC91 blends with from 0% to 100% of PMMA. The behavior is probably explained by reaching maximum of total interfaces between crystalline and amorphous regions. It can be demonstrated by DSC test. In Figure 3.4.1, melting peaks become wider as PMMA content increased from 20% to 40%. It means crystalline region is becoming smaller. But at 50% of PMMA, the melting peak disappeared which indicated that PMMA-VC91 blends were generally amorphous. It is also possible that crystal region became very small and melting peaks were too wide to be observed. The behavior of special dielectric properties

of PMMA-VC91 blends with 50% to 70% of PMMA in high temperature can be explained by above discussion that the crystalline region became very tiny so that the total interfaces between crystalline and amorphous regions approach very large value and it reached maximum when blends with 60% of PMMA. Therefore, this behavior disappeared after adding more than 70% of PMMA can be explained that all the crystalline regions of VC91 are converted into amorphous state of VC91.

The third part is blends with 80% to 100% of PMMA, shapes of Figure 3.2.11, 3.2.12 and 3.2.13 are similar due to the domination of PMMA. The dielectric constant decreases and peaks of dielectric loss increase with increase of PMMA content from 80% to 100%, due to the reduction of VC91. The peaks of dielectric loss in high temperature range caused by relaxation process associated with glass transition of PMMA-VC91 blends which was mentioned before, were gradually moved out of testing temperature. The dielectric constant in high temperature was decreased with PMMA content due to the same reason. Therefore, the curves of dielectric constant and loss of blends with from 70% to 100% of PMMA were gradually approaching the curve of pure PMMA. The dielectric properties of pure PMMA as Figure 3.2.13 were due to the relaxation process of PMMA attributed to motion of partial group chains of PMMA below glass transition temperature of PMMA [21].

3.3 Study of polarization-electric field hysteresis loops

3.3.1 P-E loops for PMMA-VC91 blends

Polarization-electric field (P-E) loops were measured under 100 Hz shown in Figure 3.3.1 to 3.3.14. The electric fields were gradually increased with 20 MV/m to the breakdown field. The results showed that the area of P-E loops and maximum polarization were increased with the increase of applied electric fields. Obviously, the value of polarization was gradually decreased with adding more PMMA content at same electric field and the breakdown field of PMMA-VC91 blends were gradually increased with the increase of PMMA content. The loops of pure VC91 were very wide because of its ferroelectricity, but the loops of pure PMMA were almost linear due to non-polar materials.

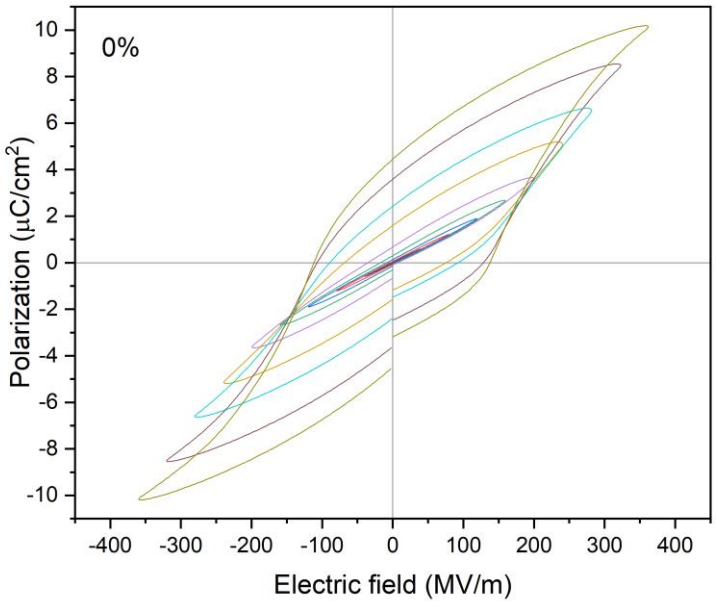

Figure 3.3. 1 P-E loops of pure VC91

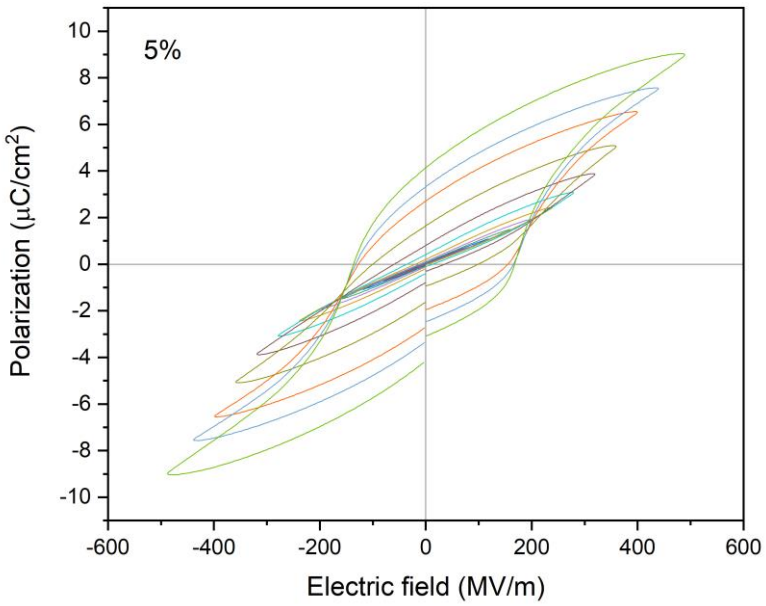

Figure 3.3. 2 P-E loops of PMMA-VC91 with 5% of PMMA

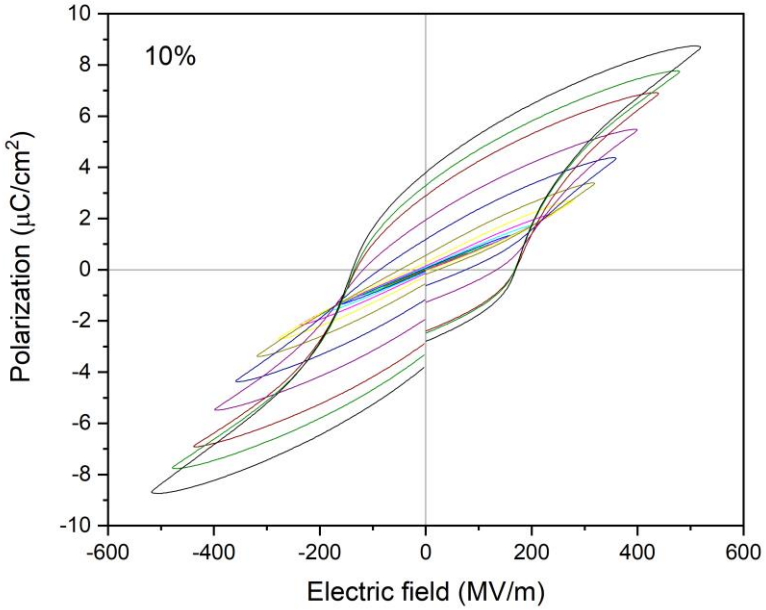

Figure 3.3. 3 P-E loops of PMMA-VC91 with 10% of PMMA

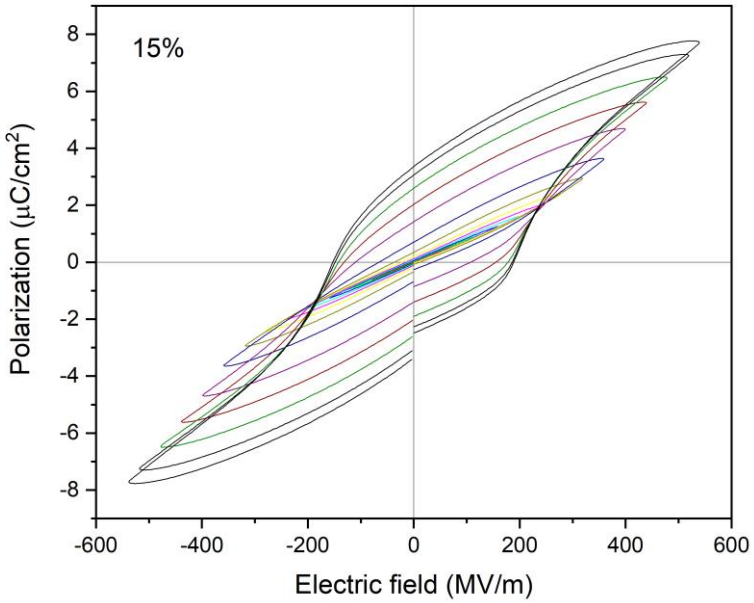

Figure 3.3. 4 P-E loops of PMMA-VC91 with 15% of PMMA

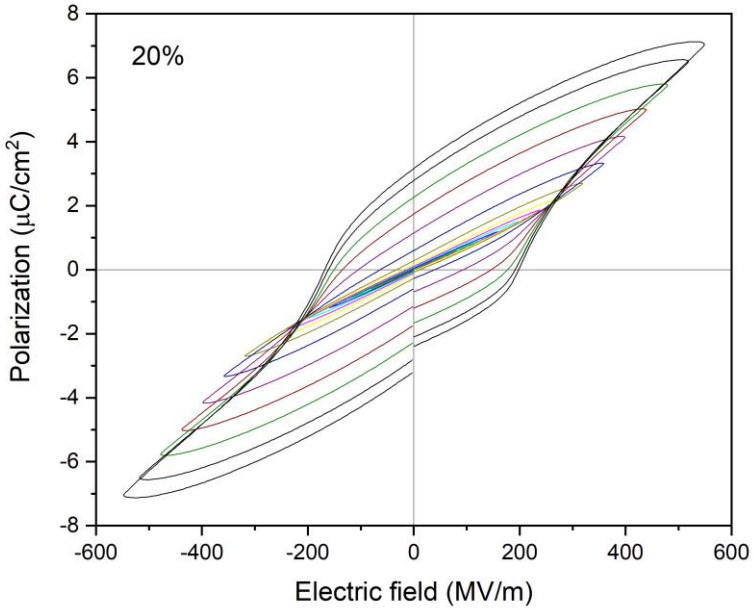

Figure 3.3. 5 P-E loops of PMMA-VC91 with 20% of PMMA

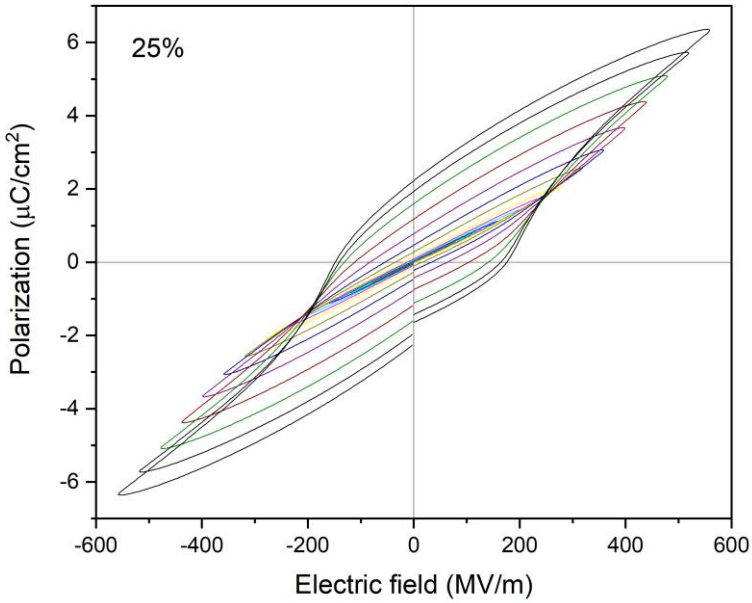

Figure 3.3. 6 P-E loops of PMMA-VC91 with 25% of PMMA

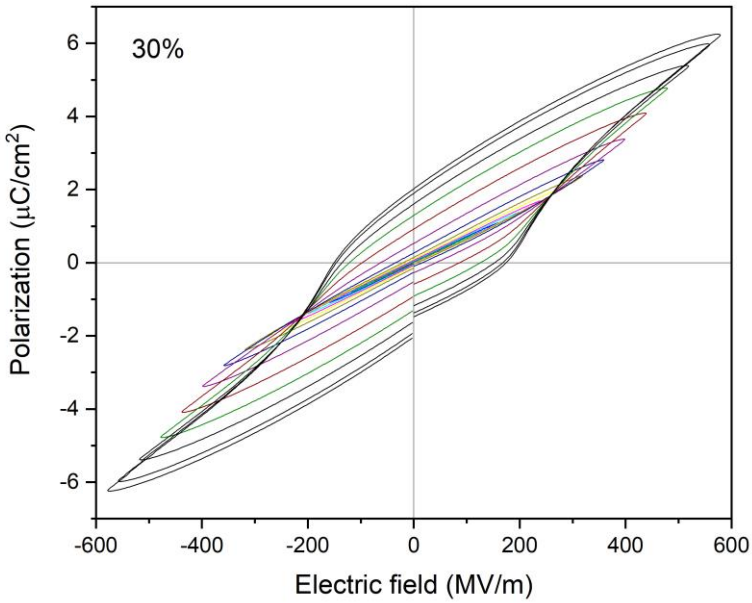

Figure 3.3. 7 P-E loops of PMMA-VC91 with 30% of PMMA

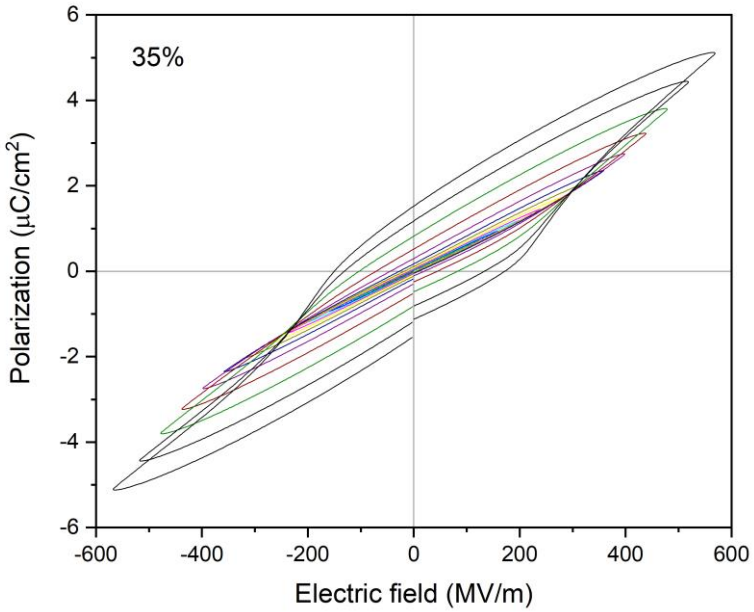

Figure 3.3. 8 P-E loops of PMMA-VC91 with 35% of PMMA

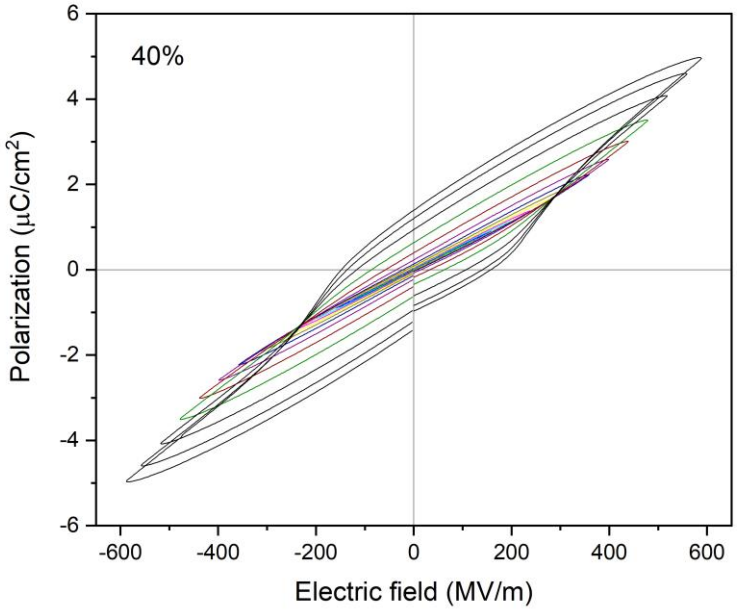

Figure 3.3. 9 P-E loops of PMMA-VC91 with 40% of PMMA

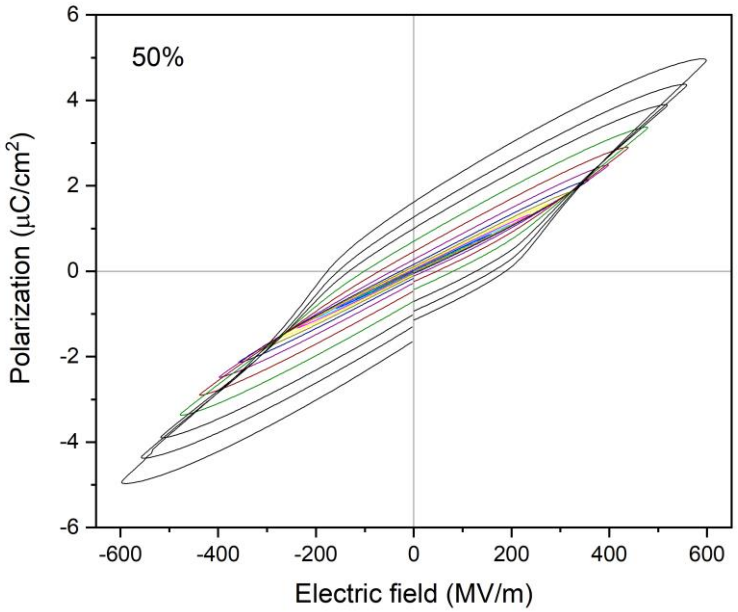

Figure 3.3. 10 P-E loops of PMMA-VC91 with 50% of PMMA

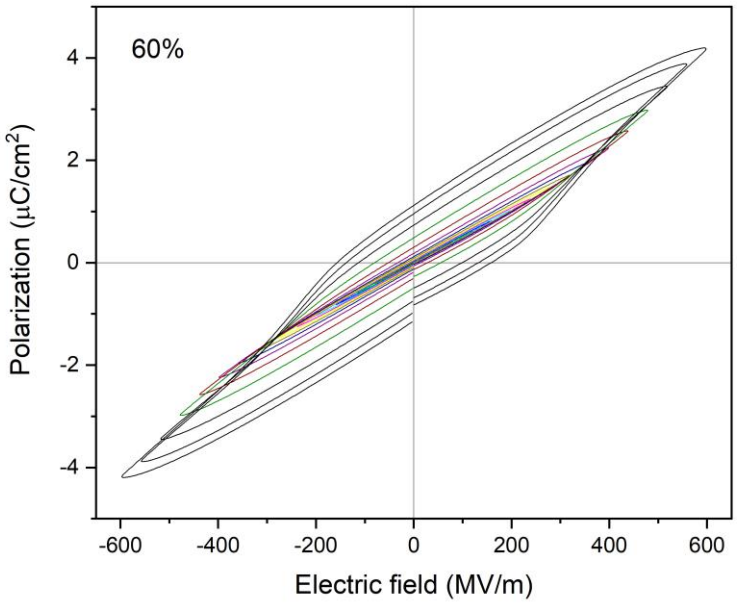

Figure 3.3. 11 P-E loops of PMMA-VC91 with 60% of PMMA

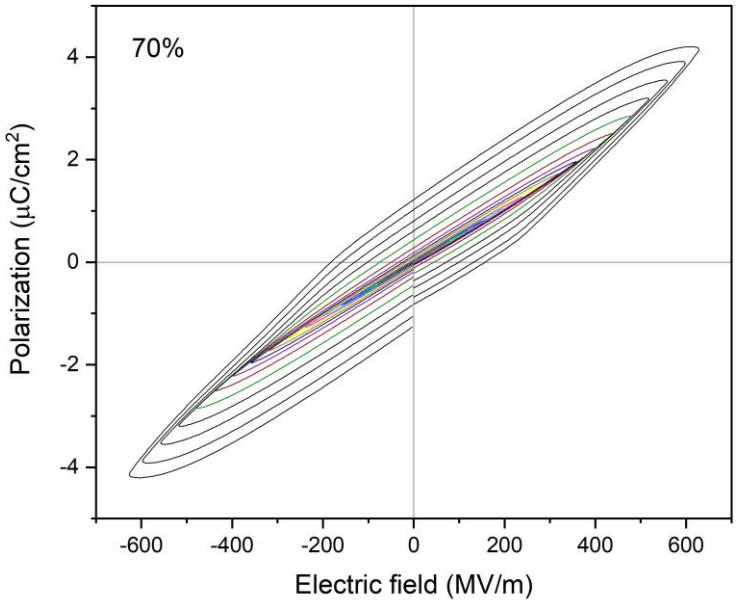

Figure 3.3. 12 P-E loops of PMMA-VC91 with 70% of PMMA

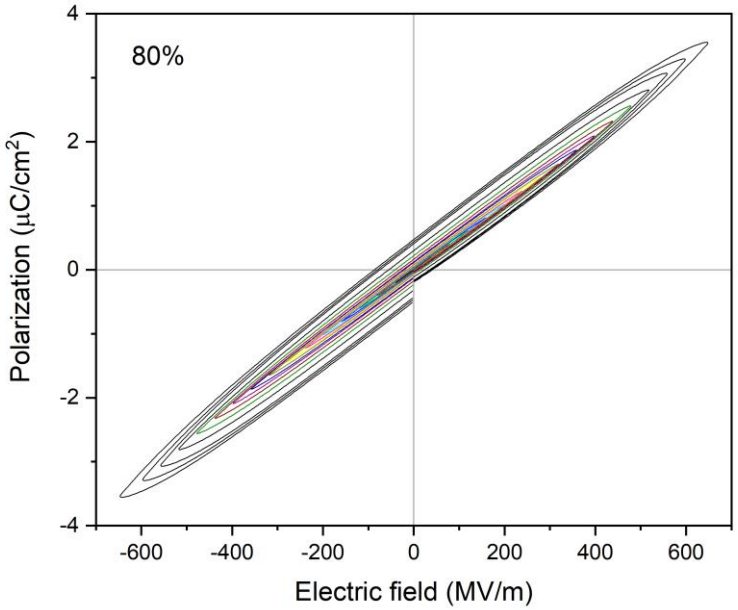

Figure 3.3. 13 P-E loops of PMMA-VC91 with 80% of PMMA

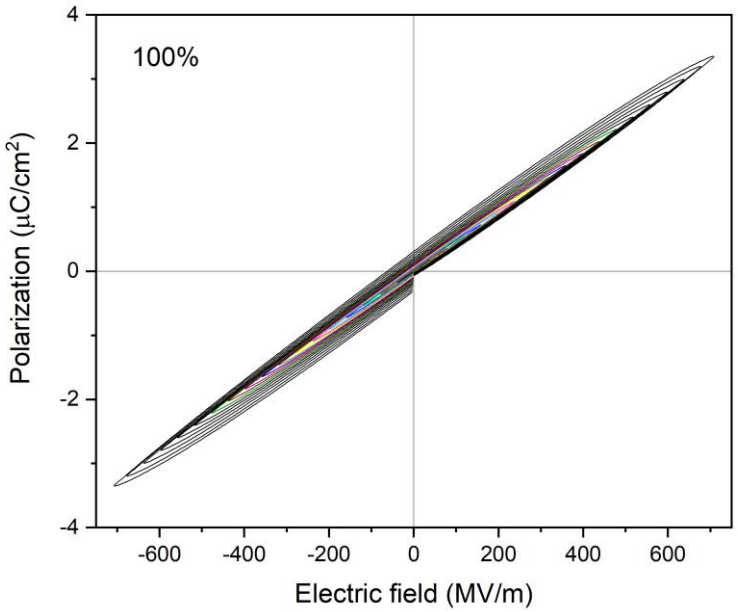

Figure 3.3. 14 P-E loops of pure PMMA

3.3.2 Breakdown fields for PMMA-VC91 blends

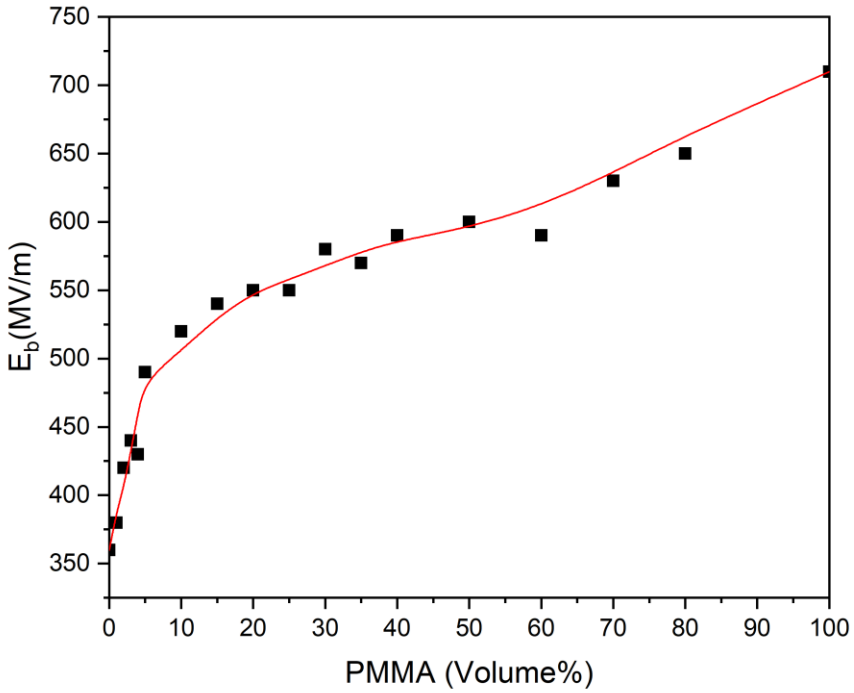

Figure 3.3. 15 Breakdown field of PMMA-VC91 as a function of volume % of PMMA

The breakdown fields which are also called dielectric strength that is the maximum electric field on the samples were shown in Figure 3.3.15. It is clear breakdown fields were increased with the increase of PMMA content. The breakdown fields were dramatically increased within 5 vol. % of PMMA. The pure PMMA had breakdown field 360 MV/m and PMMA-VC91 blend with 5% of PMMA had breakdown field 490 MV/m. Blends with 5% to 100% of PMMA had almost linear relationship between breakdown field and PMMA content. The breakdown field of pure PMMA reached maximum with 710 MV/m.

3.3.3 Study of P_{max} and P_r for PMMA-VC91 blends

The maximal polarization (P_{max}) and the remnant polarization (P_r) were shown as function of electric fields in Figure 3.3.16 and 3.3.17. The slope of P_{max} was increased with increase of electric filed for same composition of samples. The slopes and values of P_{max} was gradually decreased with increase of PMMA content. The maximum values of polarization of PMMA-VC91 blends with 0%, 5%, 10%, 15%, 20%, 25%, 30%, 35%, 40%, 50%, 60%, 70%, 80% and 100% are about 10.2, 9.0, 8.7, 7.8, 7.1, 6.3, 6.2, 5.1, 5.0, 4.9, 4.2, 4.1, 3.5 and 3.3 μC/cm^2.

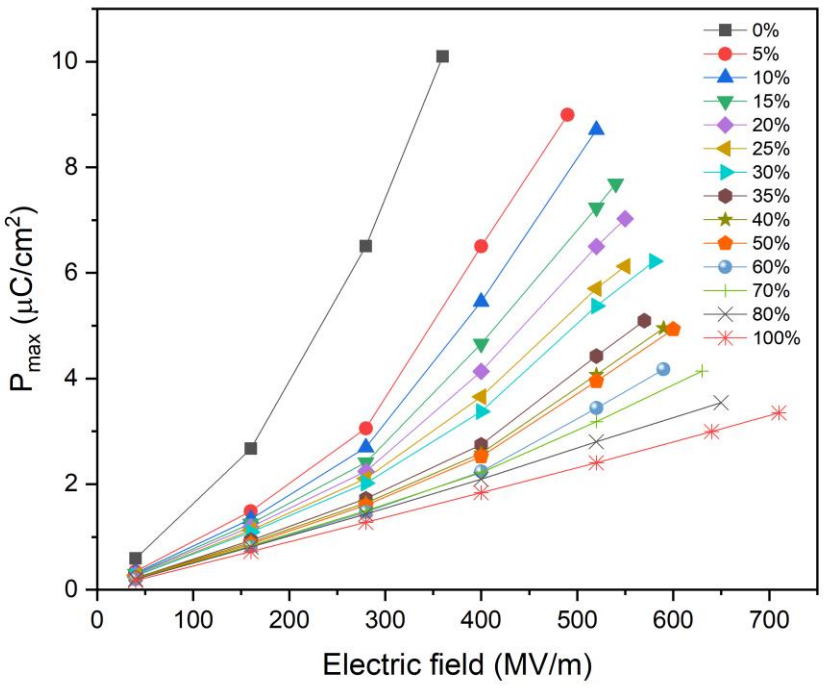

Figure 3.3. 16 P_{max} as a function an electric field with different volume % of PMMA

The slopes of P_r had similar trends with P_{max} we discussed above that were increased with increase of electric filed at same composition and slopes of P_r was gradually decreased with increase of PMMA content. But there were significant changes of slopes for each composition of samples at low applied electric fields. For example, slopes of pure VC91 and blend with 10% of PMMA were changed drastically above about 160 MV/m and 280 MV/m. The phenomenon can be explained by electric domain in ferroelectric materials. The P_r of PMMA-VC91 blends with 0%, 5%, 10%, 15%, 20%, 25%, 30%, 35%, 40%, 50%, 60%, 70%, 80% and 100% under breakdown fields are about 4.4, 4.1, 3.8, 3.4, 3.2, 2.2, 2.0, 1.5, 1.4, 1.6, 1.1, 1.2, 0.5 and 0.3 $\mu C/cm^2$, respectively.

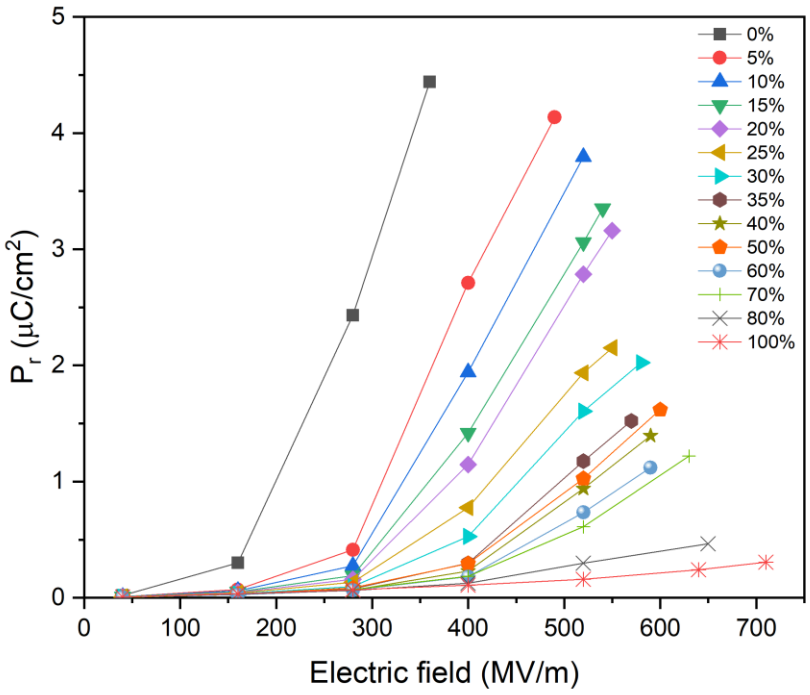

Figure 3.3. 17 P_r as a function an electric field with different volume % of PMMA

3.3.4 Energy-storage density of PMMA-VC91 blends

The energy-storage density (U) was defined by equation (1-9) as we discussed in section 1.4, and the areas in Figure 1.6 express meaning of the equation to calculate energy-storage density. The polarization $\vec{P}$ can be regarded as electric displacement $\vec{D}$ because dielectric constant of materials is much larger than 1. Therefore, P-E loops were used to calculate the areas between charge/discharge curves and y-axis (polarization axis) to evaluate the charged/discharged energy-storage density.

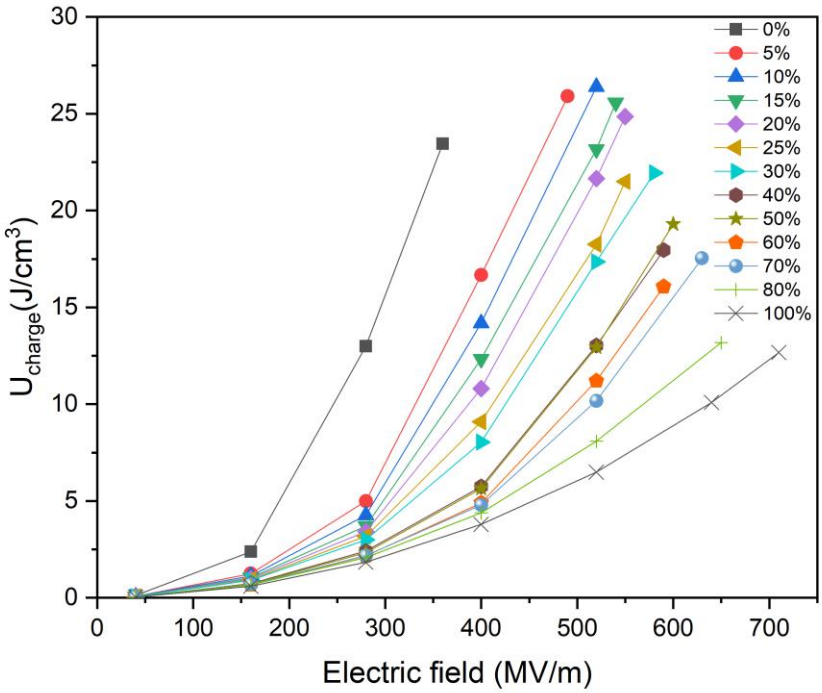

Figure 3.3. 18 U_{charge} as a function an electric field with different volume % of PMMA

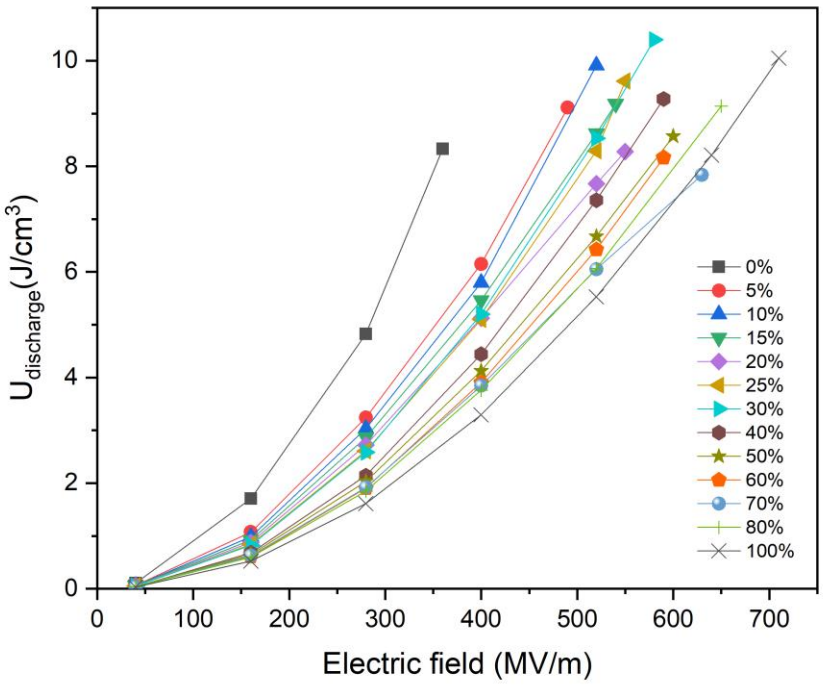

Figure 3.3. 19 $U_{discharge}$ as a function an electric field with different volume % of PMMA

The charged energy-storage density (U_{charge}) is shown as a function of electric fields as Figure 3.3.18. The slopes deceased with increase of PMMA content, which means blends with more VC91 content had larger charged energy than that with low VC91 content. The PMMA-VC91 blend with 10% of PMMA had maximum charged energy, which is about 26.4 J/cm^3. It is larger than pure VC91 which is around 23.4 J/cm^3. The pure PMMA had lowest energy charged about 12.7 J/cm^3. The result indicated charged energy is determined by both breakdown field and polarization, in other word, it is related to content of VC91 and PMMA, because adding VC91 increases polarization and adding PMMA increases breakdown field.

The discharged energy-storage density ($U_{discharge}$) is shown in Figure 3.3.19 as a function of applied fields. The curves of discharged energy density have similar shape with the curves of charged energy we discussed above. It is clear the addition of PMMA into VC91 enhanced the maximum of discharged energy-storage density due to increase of breakdown field and decrease of energy loss. The 30% of PMMA in blends reached the highest discharged energy density which was about 10.4 J/cm^3. However, the slopes of curves for PMMA-VC91 blends were smaller than that of pure VC91, especially higher volume fraction of PMMA obtained lower slopes of blends, which can be attributed to PMMA have relatively low dielectric constant compared with VC91.

Efficiency (η) is defined by $U_{discharge}/U_{charge}$ of PMMA-VC91 blends under certain applied electric field. The relationship between efficiency and electric fields with different volume fraction of PMMA in VC91 had been plotted as Figure 3.3.20. It can be found that efficiency decreases with the increase of applied fields for each sample. Roughly speaking, the efficiencies were enhanced by adding more PMMA content under a certain field. But within about 200 MV/m, the blends with addition of PMMA had higher efficiency than both pure VC91 and pure PMMA and the blend with 40% of PMMA had highest efficiency. It indicated that PMMA-VC91 blends had better efficiency than each pure polymer under low electric field. Comparing blends with different compositions at same electric fields, efficiency increase with increase of PMMA content, which is attributed to the low loss of PMMA. The increase of efficiency with addition of PMMA was more obvious under low electric fields. For instance, at 280 MV/m, the efficiency of pure VC91

was largely increased by adding 5% of PMMA from about 37% to 65%. The possible reason is that the ferroelectricity of VC91 are repressed by PMMA, so that the loss was reduced.

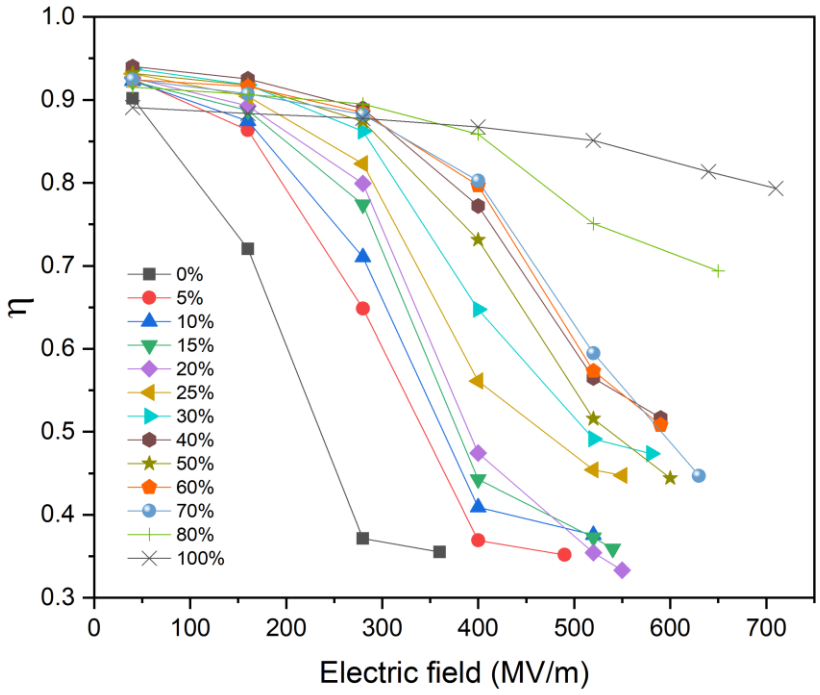

Figure 3.3. 20 Efficiency as a function an electric field with different volume % of PMMA

3.4 Study of DSC test

3.4.1 Cooling process of DSC for PMMA-VC91 blends

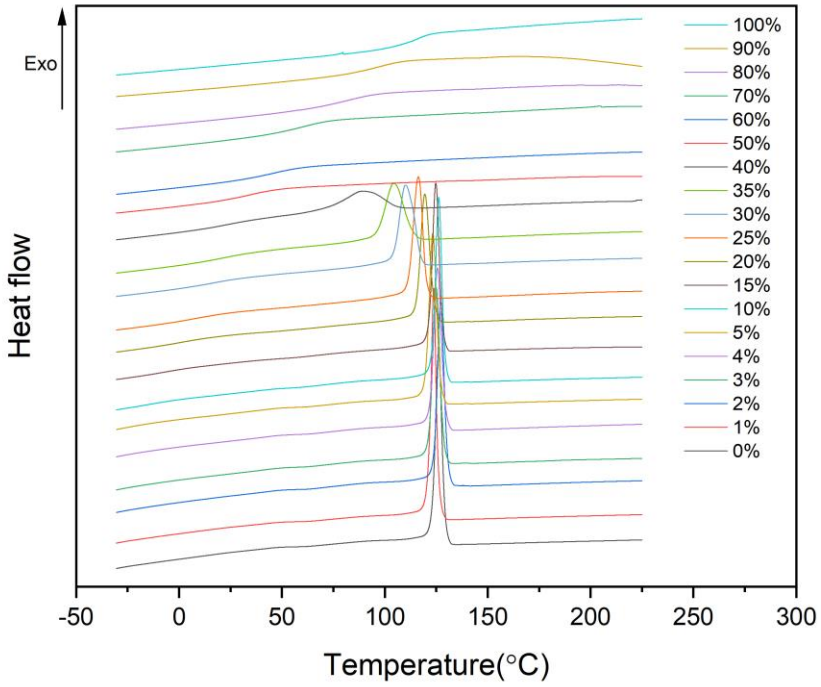

Figure 3.4. 1 The cooling process of DSC for PMMA-VC91 blends with different volume fraction of PMMA

DSC was also tested to characterize the thermal properties of PMMA-VC91 blends. Figure 3.4.1 was the plot of first cooling process of the DSC test. The samples were first heated from -90℃ to 250℃ and then chilled from 250℃ to -90℃ with 10℃ per minute. The curves of PMMA-VC91 blends with from 0% to 40% of PMMA content exhibited single peaks which was crystallization temperature for each composition of blends. The peak temperature and enthalpy for each peak were plotted as Figure 3.4.2. The peak shift toward lower temperature and the enthalpy

reduction of PMMA-VC91 blends with increase of PMMA content indicated the suppression caused by addition of PMMA which reduced the rate of crystallization and sizes of crystalline VC91[23]. It is no doubt that the decrease of enthalpy was attributed to reduction of crystallinity because fewer crystals were formed to release less heat. The peaks shifted to lower temperature and the peaks were widened, which can be attributed to smaller crystal sizes because smaller crystals had larger surface energy so that crystallization temperature became lower. The blends with more than 40 vol. % of PMMA were not plotted in Figure 3.4.2 because the crystallization peaks were not obvious, which does not mean no crystal in blends and there may be some tiny crystals which was mentioned in previous section. The crystallization peaks were not observed but a glass transition was more obvious in the blends with adding more than 40% of PMMA. The glass transition temperature of blend with 50% of PMMA was about 25℃ and the glass transition temperature shifted to higher temperature, until the glass transition temperature was about 105℃ which was the glass transition temperature of pure PMMA. The shift was attributed to miscible PMMA-VC91 blends with the increase of PMMA content we discussed before. The glass transition temperature of pure PMMA was around 105℃ which was well matched with previously well-known studies. The appearance of glass transition of blends with above 40% of PMMA was because both the crystallization peaks became weak and more miscible PMMA-VC91 sections were formed. The behaviors of glass transition of blends proved our previous explanation of the relaxation in studies of temperature dependence.

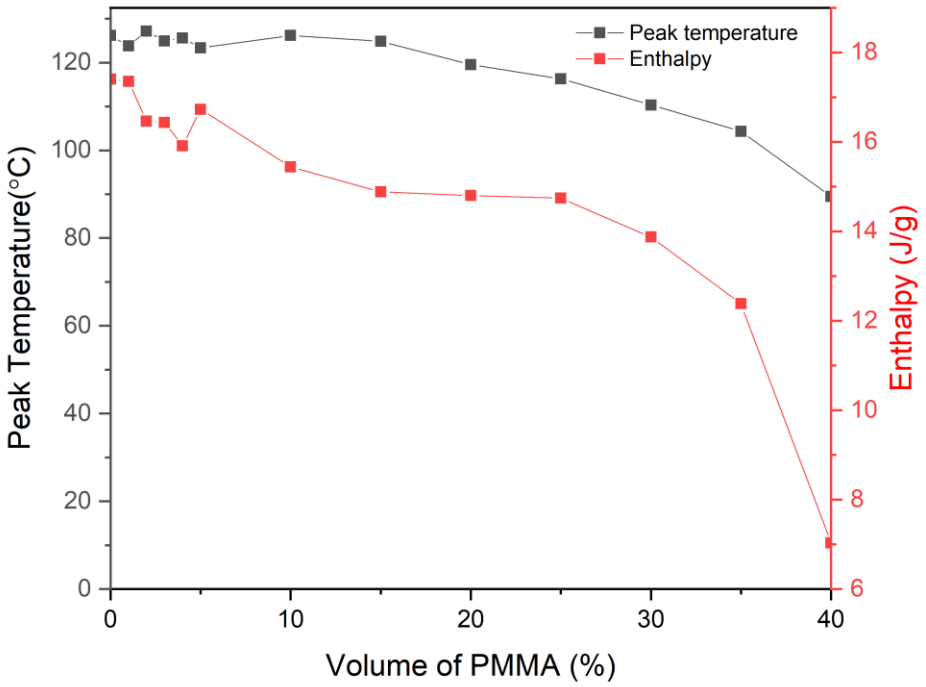

Figure 3.4. 2 Peak temperature and enthalpy in the cooling process of DSC for PMMA-VC91 blends with different volume fraction of PMMA

3.4.2 Heating process of DSC for PMMA-VC91 blends

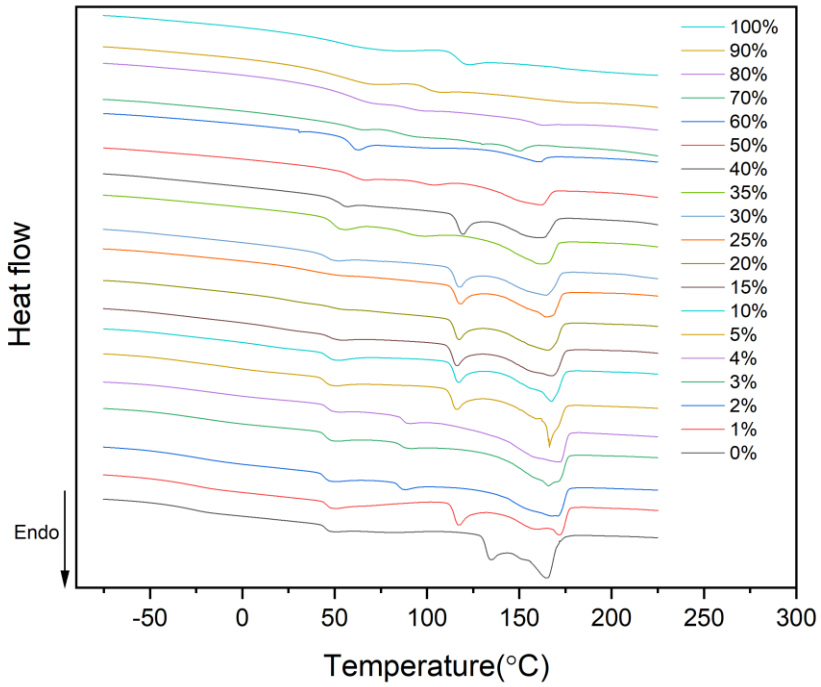

Figure 3.4. 3 The heating process of DSC for PMMA-VC91 blends with different volume fraction of PMMA

The plot of heat flow versus temperature in the heating process of DSC was shown in Figure 3.4.3 with 0% to 100% of PMMA in blends. The pure VC91 had three peaks, the first peak (peak 1) was about 50℃, the second peak (peak 2) was at 135℃ and the third peak (peak 3) was at about 170℃. The three peaks also existed in the blends with low content of PMMA and, peak temperature and enthalpy versus composition were shown in Figure 3.4.4 and 3.4.5.

The behaviors of endothermic peaks were complex and no clear so far. The peak 1 (first peak), which appeared from 0% to about 60% of PMMA in blends,

gradually moved to higher temperature shown as Figure 3.4.4. The reason of generation of peak 1 is extrinsic, probably due to moisture or ice attached on the films in VC91 content because peaks cannot see in pure PMMA and the blends with high content of PMMA. Peak1 did not show on the curves of second heating process in Figure 3.4.6 and, based on our experiences, they only occurred when a precooling step have been done before the measurement of heating process. Therefore, the first peaks may be generated by precooling process of the DSC test (DSC chamber was chilled from 40℃ to -90℃ before testing) and this behavior was related to VC91 section.

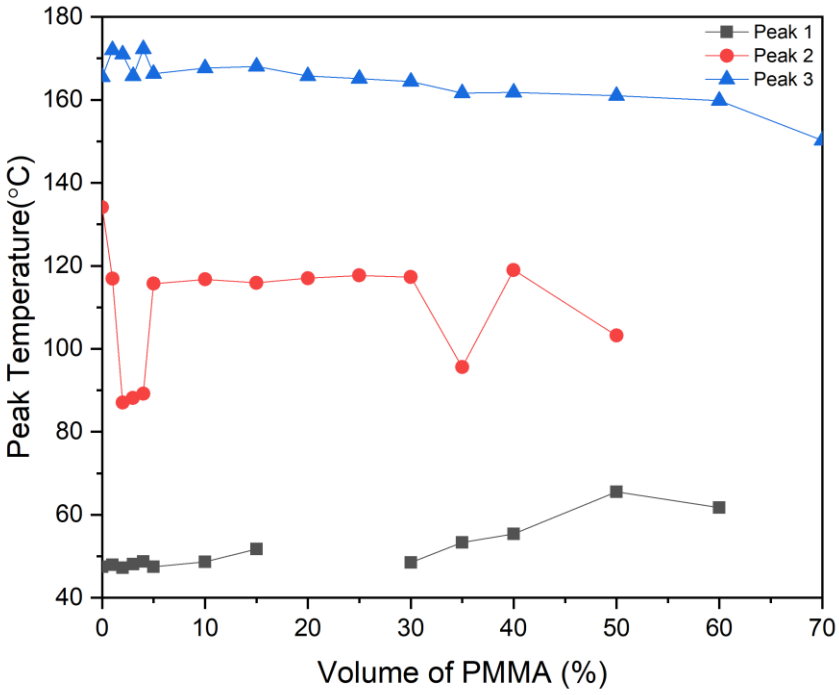

Figure 3.4. 4 Peak temperature in the Heating process of DSC for PMMA-VC91 blends with different volume fraction of PMMA

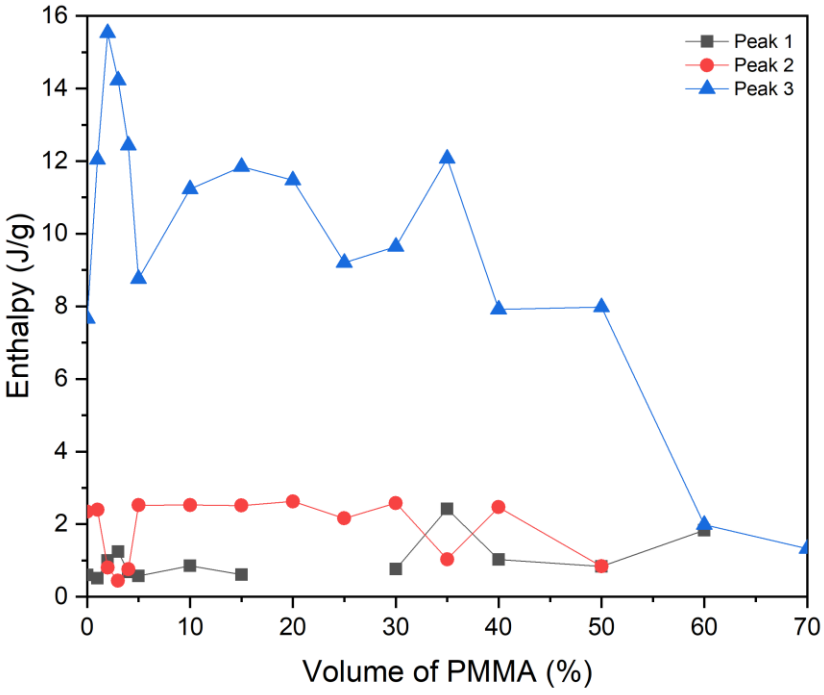

Figure 3.4. 5 Peak enthalpy in the heating process of DSC for PMMA-VC91 blends with different volume fraction of PMMA

The peak 2 and peak 3 (second peak and third peak in Figure 3.4.3) were the melting peaks of P(VDF-CTFE). The behaviors of peak 3 were clear and easily understood, which were at around 170℃ that is the characteristic of α-phase of PVDF reported in many studies [24][25]. The melting temperature of peak 3 slightly shifted to low temperature as Figure 3.4.4 due to the addition of more PMMA content. The enthalpy of peak 3 as Figure 3.4.5, roughly speaking, decreased with increase of PMMA content because of the reduction of VC91. However, the value of the enthalpy of peak 3 oscillated a lot as the increase of PMMA in Figure 3.4.5, which is because peaks were so broad that the calculation

of peaks was not very accurate, indicating that crystals of VC91 were less ordered and had large distribution of grain sizes after adding PMMA [26]. Peak 2 in Figure 3.4.3 and 3.4.4 may also be the melting peaks, which had lower temperature (about 135℃ for pure VC91, around 120℃ for blends with 1%, 5%, 10%, 15%, etc. of PMMA, approximately 90℃ for blends with 2%, 3%, 4%, 35% of PMMA). It may be attributed to incomplete crystallization of VC91 and we will further discuss it in next section.

The glass transition of pure PMMA in Figure 3.4.3 occurred at about 105℃ which was well-known by many studies and consistent with cooling process of DSC. For the blend with 90% of PMMA, the glass transition temperature was about 100℃ and the reason we discussed above. The glass transition processes of the blends with lower content of PMMA were not obvious because the change of thermal flow was too weak to be observed. For the glass transition of VC91, its temperature is about -40℃ [18] and it was not clearly observed in Figure 3.4.3 due to the weak changes of thermal flow.

3.4.3 Double test of DSC for pure VC91

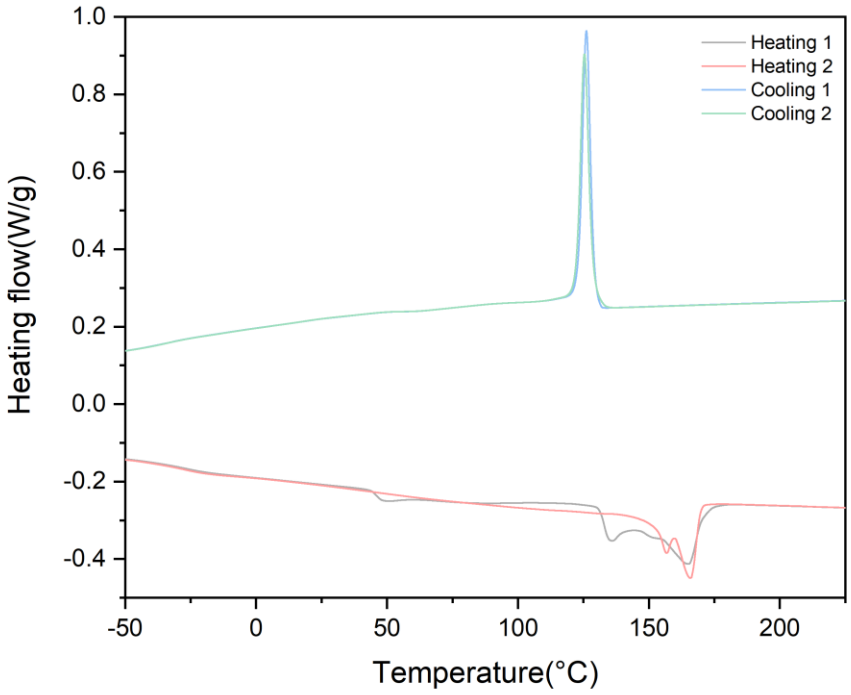

Figure 3.4. 6 Double test of DSC for VC91 film

The pure VC91 was tested by DSC with double runs as Figure 3.4.6. Two crystallization peaks in two cooling processes had same shape, temperature and enthalpy, indicating no weight loss and chemical reaction happened during heating process. In the heating process, two melting peaks approached closer in second run than that of first run, demonstrating the previous assumption of existence of two melting peaks is correct which is due to incomplete heat treatment. Therefore, current 140℃ annealing was not enough to get complete crystallization process, so a higher annealing temperature and a longer time might achieve better dielectric properties for PMMA-VC91 blends.

CHAPTER 4

CONCLUSIONS AND FUTURE WORK

4.1 Conclusions

Transparent and flexible PMMA-VC91 blends were successfully fabricated by spin-coating method with different volume fraction of PMMA. Obtained films with about 8 microns show the great uniformity. Dielectric properties at room temperature were characterized and it showed that dielectric constant decreased with increase of PMMA content. Dielectric loss at room temperature decreased at low frequency (from 100 Hz to 10k Hz) and increased at high frequency (from 10k Hz to 1M Hz), with increase of PMMA content. The temperature dependence of dielectric properties was also studied in order to understand the thermal stability of PMMA-VC91 blends. Several new relaxation processes related to motion of polymer chains and interface between crystal and amorphous regions, were occurred and used to explain the thermal dielectric phenomena in high temperature. Polarization-electric field hysteresis loops were measured which indicated maximal polarization of blends decreased with addition of PMMA. Also, blends with higher volume fraction of PMMA obtained higher breakdown fields. Charged and discharged energy-storage density and efficiency were calculated from P-E loops, indicating blend with 10 vol. % of PMMA had maximum charged energy density which is about 26.4 J/cm^3, blend with 30 vol. % of PMMA had maximum discharged energy density about 10.4 J/cm^3. The addition of PMMA in blends dramatically increased efficiency of discharged/charged energy density. The

thermal behaviors of PMMA-VC91 blends were characterized by DSC for better understanding the influence of the crystalline forms and glass transition on the dielectric behaviors of PMMA-VC91 blends.

4.2 Future work

The current characterization and studies so far generally understood the dielectric properties and energy storage of PMMA-VC91 blends. However, some assumption and explanation we discussed still need more evidences to demonstrate. Other characterization methods, such as XRD and FTIR, may give us more information to further understand the dielectric properties and to prove some current assumptions. The results of DSC test were complex and not clear, showing that the crystalline process of our PMMA-VC91 blends was not fully complete. A higher annealing temperature should be used to make a better crystalline of blends. But, PMMA-VC91 blends were partially melted with a heat treatment above 140°C, which influenced the quality of films to do further measurements of dielectric properties. Therefore, an optimal method of heat treatment should be found to obtain PMMA-VC91 blends with full crystallization.

REFERENCES

[1] Kao, Kwan Chi. Dielectric phenomena in solids. Elsevier, 2004.

[2] Rao, Yang, et al. "Novel polymer–ceramic nanocomposite based on high dielectric constant epoxy formula for embedded capacitor application." Journal of Applied Polymer Science 83.5 (2002): 1084-1090.

[3] Zhang, L. I. N., and Z-Y. Cheng. "Development of polymer-based 0–3 composites with high dielectric constant." Journal of Advanced Dielectrics 1.04 (2011): 389-406.

[4] Hummel, Rolf E. Electronic properties of materials. Springer Science & Business Media, 2011.

[5] Irodov, Igor′ Eugen′evich, Natasha Deineko, and Ram Wadhwa. Basic laws of electromagnetism. Imported Pubn, 1986.

[7] Wang, Wei. Novel Metal-Polymer Composite with High Percolation Threshold. Diss. 2012.

[8] Shan, Xiaobing. High dielectric constant 0-3 ceramic-polymer composites. Auburn University, 2009.

[9] Zheng, Jim P. "Dielectric properties of PVDF films and polymer laminates with PVDF for energy storage applications." Proceedings of the 6th International Conference on Properties and Applications of Dielectric Materials (Cat. No. 00CH36347). Vol. 1. IEEE, 2000.

[10] Chen, Lin-Feng, et al. Microwave electronics: measurement and materials characterization. John Wiley & Sons, 2004.

[11] Zhang, Lin. Fundamental study and development of 0-3 dielectric composites with high dielectric constant. Diss. 2013.

[12] Lu, Xu, et al. "Dielectric and energy-storage performance of Ba0. 5Sr0. 5TiO3-SiO2 ceramic-glass composites." Journal of Alloys and Compounds 745 (2018): 127-134.

[13] Chu, Baojin, et al. "A dielectric polymer with high electric energy density and fast discharge speed." Science 313.5785 (2006): 334-336.

[14] Meng, Qingjie, et al. "Effect of poly (methyl methacrylate) addition on the dielectric and energy storage properties of poly (vinylidene fluoride)." Journal of applied polymer science 116.5 (2010): 2674-2684.

[15] Zhao, Xiaojia, et al. "Exploring the relationship of dielectric relaxation behavior and discharge efficiency of P (VDF-HFP)/PMMA blends by dielectric spectroscopy." Materials Research Express 3.7 (2016): 075304.

[16] Lu, Xu, Yang Tong, and Z-Y. Cheng. "Fabrication and characterization of free-standing, flexible and translucent BaTiO3-P (VDF-CTFE) nanocomposite films." Journal of Alloys and Compounds 770 (2019): 327-334.

[17] Lu, Xu, et al. "BST-P (VDF-CTFE) nanocomposite films with high dielectric constant, low dielectric loss, and high energy-storage density." Composites Part B: Engineering 168 (2019): 34-43.

[18] Mandelkern, L., G. M. Martin, and F. A. Quinn. "Glassy state transitions of poly-(chlorotrifluoroethylene), poly-(vinylidenefluoride), and their copolymers." J. Res. Nat. Bur. Stand 58 (1957): 137-143.

[19] Schadler, Linda. "Nanocomposites: model interfaces." Nature materials 6.4 (2007): 257.

[20] Lu, Xu, et al. "Dielectric property and ac conductivity of P (VDF-CTFE)-PLZST polymer-ceramic composite films." Ceramics International (2019).

[21] Li, Chaoxu, et al. "Effect of inorganic phase on polymeric relaxation dynamics in PMMA/silica hybrids studied by dielectric analysis." European polymer journal 40.8 (2004): 1807-1814.

[22] Liu, Jinhui, et al. "Effect of electronegativity and steric hindrance of the cocatalyst on the activity and selectivity of butadiene polymerization catalyzed by molybdenum." Journal of Applied Polymer Science 136.1 (2019): 46906.

[23] Chu, Huiying, et al. "Enhancing released electrical energy density of poly (vinylidene fluoride-co-trifluoroethylene)-graft-poly (methyl methacrylate) via the pre-irradiation method." Applied Surface Science 465 (2019): 643-655.

[24] Campos, Joao Sinezio de C., Alexandre A. Ribeiro, and Celso Xavier Cardoso. "Preparation and characterization of PVDF/CaCO3 composites." Materials Science and Engineering: B 136.2-3 (2007): 123-128.

[25] Benedetti, Enzo, et al. "FTIR-microspectroscopy and DSC studies of poly (vinylidene fluoride)." Polymer international 41.1 (1996): 35-41.

[26] Li, Zhimin, Milind D. Arbatti, and Z-Y. Cheng. "Novel electroactive polymer system: PVDF-based polymer blends." Smart Structures and Materials 2004: Electroactive Polymer Actuators and Devices (EAPAD). Vol. 5385. International Society for Optics and Photonics, 2004.